

Anorganische Chemie

Prof. Dr. Claudia Felser

Die Forschungsaktivitäten der *Moment-Gruppe* (MOMENT = Materialien für optische, magnetische und Energie-Technologien) liegen an der Schnittstelle zwischen Festkörperchemie, Werkstoffforschung und Physik kondensierter Materie. Daher umfasst die Gruppe Physiker, Chemiker und Materialwissenschaftler, die an der Synthese neuer Materialien für interdisziplinäre Forschungsfelder wie z. B. Spintronik oder Materialien zur Energieumwandlung arbeiten.

Die allgemeine Forschungsphilosophie der Gruppe ist die rationale Planung von neuen multifunktionalen Materialien unter Verwendung vorhersagender theoretischer Simulationen sowie die Herstellung dieser Stoffe unter Einsatz modernster Methoden zur Synthese und Charakterisierung. Forschungsgegenstand sind Heusler-Verbindungen der Zusammensetzung X_2YZ mit dem Strukturtyp $L2_1$ sowie Halb-Heusler-Verbindungen der Zusammensetzung XYZ mit dem $C1_b$ Strukturtyp. Sie sind eine bemerkenswerte Klasse innerhalb der intermetallischen Materialien und umfassen mehr als 1000 Verbindungen [T. Graf et al. *Progress in Solid State Chemistry* 39, 1 (2011)]. Speziell der 1:1:1 Verbindungstyp kann als eine gefüllte Variante der binären Halbleiter mit ZnS Struktur beschrieben werden. Heusler-Verbindungen zeigen die gleiche breite Eigenschaftsvielfalt wie Perowskite z. B. einstellbare magnetische Eigenschaften, Halbleitereigenschaften, große Magnetwiderstandseffekte, Supraleitung, Li-Ionenleitung und andere interessante physikalische Eigenschaften.

Dabei werden weitere neue Eigenschaften und mögliche Anwendungsfelder immer wieder entdeckt: eines der jüngsten Beispiele ist die Vorhersage von topologischen Isolatoren [S. Chadov et al., *Nature Mat.* 9, 541 (2010), siehe Reporte *A Recipe for Topological Insulators* (Seite 228), und *Electronic Structure of Heusler Compounds with $C1_b$ Structure and "Zero Band Gap"* (Seite 232)]. Überraschenderweise können die Eigenschaften vieler Heusler-Verbindungen allein schon aus der Anzahl der Valenzelektronen vorhergesagt werden. Ihre extrem flexible kristallo-

graphische und elektronische Struktur öffnet einen Werkzeugkasten, welcher die Realisierung von gewünschten, sogar manchmal widersprüchlichen Funktionalitäten in einer Verbindung ermöglicht.

Bauelemente, die auf multifunktionalen Eigenschaften beruhen, d. h. die Kombination von zwei oder mehr Funktionen wie Supraleitung und topologische Oberflächenzustände, führen nicht nur zu neuen Quanteneffekten, sondern können eventuell in Zukunft technische Anwendungen revolutionieren [siehe Report *A Recipe for Topological Insulators* (Seite 228)]. Die Untergruppe der Halb-Heusler-Verbindungen mit mehr als 250 Halbleitern besitzt eine große Bedeutung für die Entwicklung von neuen Materialien für erneuerbare Energietechnologien. Bandlücken von 0 bis 4 eV können durch Änderung der chemischen Zusammensetzung eingestellt werden. Sowohl im Bereich des Designs neuer Solarzellen [S. Sakurada and N. Shutoh, *Appl. Phys. Lett.* 86, 082105 (2005), S. Ouardi, et al., *Appl. Phys. Lett.* 97, 252113 (2010). Patent Martin Köhne et al., published 15.12.2010, DE 10 2010 029 968] als auch neuer thermoelektrischer Materialien [D. Kieven et al., *Phys. Rev. B* 81, 075208 (2010), D. Kieven et al., *Thin Solid Films* 519, 1866 (2011); Claudia Felser et al., Filing Date: November 18, 2010; US 61/415,266] gibt es großes Interesse der Industrie. Wir arbeiten mit BASF, Bosch und anderen Firmen an der Entwicklung thermoelektrischer Bauteile basierend auf Halb-Heusler-Verbindungen zusammen und mit IBM, Schott, Bosch, Stanford and National Renewable Energy Laboratory (NREL), Boulder USA, an der Entwicklung von neuen Solarzellen. Außer im Hinblick auf den „hohen thermoelektrischen Gütefaktor“ lassen sich Halb-Heusler-Verbindungen unter für die Industrie wichtigen Gesichtspunkten wie geringe Kosten, Verfügbarkeit, Nichtgiftigkeit und einfache Prozessführung herstellen. Das NREL-Labor hat vor Kurzem – angeregt durch unsere Forschungsaktivitäten – das Energy Frontier Research Center (<http://www.centerforinversedesign.org>) mit dem Thema „filled tetrahedral structures for solar cell

Inorganic Chemistry

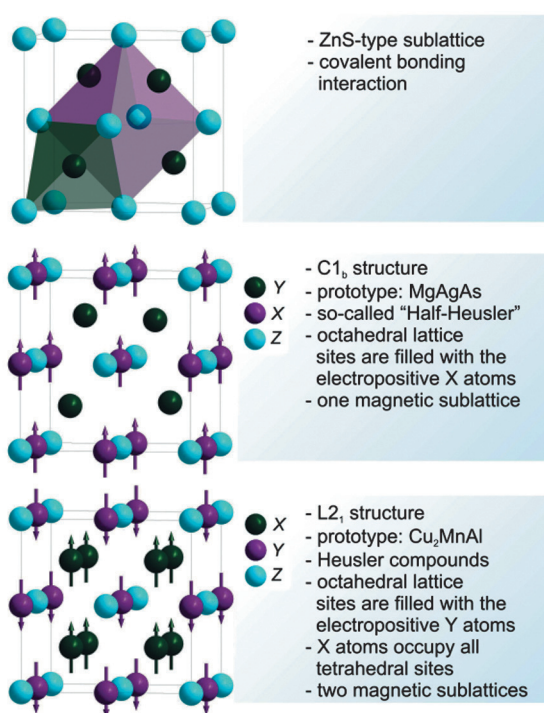
Prof. Dr. Claudia Felser

The research activities of the *Moment group* (MOMENT = Materials for Optical, Magnetic and Energy Technologies) are at the interface between solid state chemistry, materials science, and condensed matter physics. The group comprises physicists, chemists, and materials scientists and focuses on synthesis of new materials for interdisciplinary research fields such as spintronics and materials for energy conversion.

The overall research philosophy is the rational design of new multifunctional materials combining state-of-the-art synthesis and characterization with predictive theoretical simulations. In general the material class under investigation – Heusler compounds X_2YZ with $L2_1$ and Half-Heusler compounds XYZ with $C1_b$ structure type – show the same broad variety of properties as the perovskites, including tunable magnetic properties, semiconductivity, magnetoresistance effects, superconductivity, Li-ion-conductivity and other physical properties. Heusler compounds are a remarkable class of intermetallic materials comprising more than 1000

members [T. Graf et al. *Progress in Solid State Chemistry* 39, 1 (2011)]. Especially the 1:1:1 compound can be understood as a stuffed version of the binary semiconductors with ZnS structure.

New properties and potential fields of applications emerge constantly; the prediction of topological insulators is the most recent example [S. Chadov et al., *Nature Mat.* 9, 541 (2010); see reports *A Recipe for Topological Insulators* (page 228), and *Electronic Structure of Heusler Compounds with $C1_b$ Structure and “Zero Band Gap”* (page 232)]. Surprisingly, the properties of many Heusler compounds can easily be predicted by the valence electron count. Their extremely flexible crystal and electronic structure offers a toolbox, which allows the realization of demanded but sometimes contradictory functionalities within one ternary compound. Devices based on multifunctional properties, i.e. the combination of two or more functions such as superconductivity and topological edge states will revolutionize technological applications [see report *A Recipe for Topological Insulators* (page 228)]. The sub-group of more than 250 semiconductors is of high relevance for the development of novel materials for energy technologies. Their band gaps can readily be tuned from zero to ≈ 4 eV by changing the chemical composition. Thus, great interest has been attracted in the fields of thermoelectric [S. Sakurada and N. Shutoh, *Appl. Phys. Lett.* 86, 082105 (2005), S. Ouardi, et al., *Appl. Phys. Lett.* 97, 252113 (2010). Patent Martin Köhne et al., published 15.12.2010, DE 10 2010 029 968] and solar cell research [D. Kieven et al., *Phys. Rev. B* 81, 075208 (2010); D. Kieven, et al., *Thin Solid Films* 519, 1866 (2011); Claudia Felser et al., Filing Date: November 18, 2010; US 61/415,266]. We are collaborating with BASF, Bosch and others on thermoelectric devices based on Half Heusler compounds and with IBM, Schott, Bosch, Stanford and National Renewable Energy Laboratory (NREL), Boulder USA on new materials for solar cells. Beside having a high figure of merit, Half-Heusler compounds are extremely flexible materials which can be designed and produced by taking industrial



applications and transparent conducting oxides (TCO's) = gefüllte Tetraeder Strukturen für Solarzellenanwendungen und transparente leitende Oxide) gegründet.

Hochenergie-Photoemission (HAXPES) ist eine neue Entwicklung, die gerade für die Festkörperforschung und zur Untersuchung von Volumenproben von Bedeutung ist [siehe Bericht *Magnetic Dichroism in Angle-Resolved Hard X-ray Photoemission from Magnetic Thin Films* (Seite 225)]. Wegen der hohen Anregungsenergie ist die Methode nicht wie die konventionelle Photoemission oberflächenempfindlich, sondern es ist sogar möglich, Grenzflächen in Funktionseinheiten zu untersuchen [siehe Report *Electronic Structure of Heusler Compounds with Cl_b Structure and "Zero Band Gap"* (Seite 232)]. Sowohl bei PETRA III in Hamburg als auch bei SPring-8 in Japan haben wir in den letzten drei Jahren weltweit zum erstenmal spinaufgelöste Hochenergie-Photoemissionsuntersuchungen durchgeführt [siehe Berichte *HAXPES: Spin Polarization, Linear and Circular Magnetic Dichroism in Angle-Resolved Hard X-ray PhotoElectron Spectroscopy* (Seite 221) und *Magnetic Dichroism in Angle-Resolved Hard X-ray Photoemission from Magnetic Thin Films* (Seite 225)].

Der weite Bereich der multifunktionalen Eigenschaften von Heusler- bzw. Halb-Heusler-Verbindungen spiegelt sich z. B. auch in den magneto-optischen, magneto-elektronischen und magneto-kalorischen Eigenschaften wieder. Das bekannteste Beispiel ist die Kombination von Magnetismus und außergewöhnlichen Transporteigenschaften in den Spintronik-Bauelementen [T. Graf, et al., *IEEE Trans. Mag.* 47, 367 (2011)]. Nahezu alle auf dem Elektroniksektor arbeitenden Unternehmen wie Hitachi, Seagate, IBM, TDK, Western Digital weisen Aktivitäten auf dem Gebiet der Spintronik mit Heusler-Verbindungen auf. Aktuell arbeiten wir mit Western Digital, Hitachi, IBM sowie mit kleinen und mittleren Firmen (Prema and Sensitec) zusammen.

Thermoelektrische Materialien

Fast alle der halbleitenden und halbmolekularen Halb-Heusler-Verbindungen sind 18-Valenzelektronen-Verbindungen (im Falle von Selten-erdmetall-haltigen Verbindungen sind die f-Elektronen so lokalisiert, dass sie nicht zu den Valenzelektronen beitragen). Halbleiter wie

CoTiSb überraschen, da diese Verbindung ausschließlich aus Metallen besteht. Halbleiter mit kleiner Bandlücke erzeugten in Japan großes wissenschaftliches Interesse aufgrund ihrer möglichen Anwendungen im Bereich der Thermoelektrika und Spintronik. Die elektronische Struktur der 18-Valenzelektronen-Verbindungen zeigt schmale Bänder von d-Elektronen, was zu einer hohen effektiven Masse und einer Thermokraft S bis zu $400 \mu\text{VK}^{-1}$ bei Raumtemperatur führt [S. Ouardi, et al., *Appl. Phys. Lett.* 97, 252113 (2010), C. Uher, J. Yang, S. Hu, D. T. Morelli, and G. P. Meisner, *Phys. Rev. B* 59, 8615 (1999)]. Ein großer Vorteil der Heusler-Verbindungen besteht in der Möglichkeit, durch individuelle Dotierung der drei (unabhängigen) besetzten fcc-Untergitter die thermoelektrischen Eigenschaften zu optimieren. Einziger Nachteil ist die relativ hohe thermische Leitfähigkeit mit Werten um die 10 W/mK . Die Verbindung $(\text{Zr}_{0.5}\text{Hf}_{0.5})_{0.5}\text{Ti}_{0.5}\text{NiSn}_{0.998}\text{Sb}_{0.002}$ zeigt bei 700 K einen maximalen intrinsischen ZT -Wert von 1.4 [S. Sakurada and N. Shutoh, *Appl. Phys. Lett.* 86, 082105 (2005)]. Für den n-Halbleiter $\text{Ti}_{0.6}\text{Hf}_{0.4}\text{Co}_{0.87}\text{Ni}_{0.13}\text{Sb}$ – basierend auf TiCoSb – wird ein ZT -Wert von 0.7 bei 900 K bei einer Thermokraft (power factor) von $23.4 \mu\text{Wcm}^{-1}\text{K}^2$ [S. Bhattacharya, et al., *Appl. Phys. Lett.* 77, 2476 (2000)] berichtet. Um die intrinsischen Eigenschaften dieser komplexen Systeme zu verstehen, haben wir eine prototypische Verbindung als Einkristall hergestellt. $\text{Zr}_{0.5}\text{Hf}_{0.5}\text{NiSn}$ -Einkristalle weisen einen hohen intrinsischen ZT -Wert von 0.4 bei 350 K auf [S. Ouardi, et al., *Appl. Phys. Lett.* 99, 152112 (2011)], was eine Gütezahl höher als 1 bei 800 K erwarten lässt. Im Allgemeinen können wir die großen ZT -Werte der japanischen Gruppen reproduzieren. In Zusammenarbeit mit Bosch haben wir herausgefunden, dass sich alle guten thermoelektrischen Verbindungen durch eine Phasenseparation / spinodale Zersetzung auszeichnen, wodurch ein feinkörniges Gefüge entsteht. Dieses ist wohl der Grund für die erniedrigte thermische Leitfähigkeit [DE 10 2010 029 968].

Multifunktionale topologische Isolatoren

Viele der Materialien mit ausgezeichneten thermoelektrischen Eigenschaften sind gleichzeitig topologische Isolatoren (topological insulator TI). Eines der ersten TI-Systeme war die Quantentopfstruktur im System $\text{CdTe}/\text{HgTe}/\text{CdTe}$. Mit den Erläuterungen in diesem Bericht ist es offensicht-

considerations into account such as low cost, sustainability, non-toxicity and easy processibility. The NREL has recently started an Energy Frontier Research Center (<http://www.centerforinversedesign.org>) on “filled tetrahedral structures for solar cell applications and transparent conducting oxides” (TCO’s) stimulated by our research.

Hard X-Ray Photoemission (HAXPES) is a new development which is extremely useful for investigation of the electronic structure of bulk materials [see report *Magnetic Dichroism in Angle-Resolved Hard X-ray Photoemission from Magnetic Thin Films* (page 225)]. With high excitation energies the escape depth of the photoelectron can be up to 100 nm, which allows even the investigation of interfaces in devices [see report *Electronic Structure of Heusler Compounds with Cl_b Structure and “Zero Band Gap”* (page 232)]. At PETRA III in Hamburg as well as in SPring-8, Japan we have built a spin-resolved HAXPES station, which allows spin-resolved HAXPES investigations for the first time, worldwide. [see report *HAXPES: Spin Polarization, Linear and Circular Magnetic Dichroism in Angle-Resolved HARD X-ray Photo Electron Spectroscopy* (page 221) and *Magnetic Dichroism in Angle-Resolved Hard X-ray Photoemission from Magnetic Thin Films* (page 225)].

The wide range of the multifunctional properties of Heusler compounds is also reflected in extraordinary magneto-optical, magneto-electronic, and magneto-caloric properties. The most prominent example is the combination of magnetism and exceptional transport properties in spintronic devices [T. Graf, et al., *IEEE Trans. Mag.* 47, 367 (2011)]. Nearly all electronic companies such as Hitachi, Seagate, IBM, TDK, Western Digital have activities in the field of spintronics with Heusler compounds. We collaborate with Western Digital, Hitachi, IBM and SMEs (small and medium enterprises) from Germany (Prema and Sensitec) in the area of spintronics.

Thermoelectric materials

The large group of semiconducting and semimetallic Half Heusler materials is formed by 18 valence electron compounds (in case of rare earth containing compounds the localized f electrons can be ignored). This leads to surprising semiconductors such as CoTiSb. These narrow band gap semiconductors have attracted great scientific interest due

to their possible application in the field of thermoelectric and spintronics in Japan. The electronic structure of the 18 valence electron compounds revealed narrow bands from the d electrons, leading to a high effective mass and a large thermopower S up to $\approx 400 \mu\text{VK}^{-1}$ at room temperature [S. Ouardi, et al., *Appl. Phys. Lett.* 97, 252113 (2010), C. Uher, J. Yang, S. Hu, D. T. Morelli, and G. P. Meisner, *Phys. Rev. B* 59, 8615 (1999)]. A great advantage of Heusler compounds is the possibility to substitute each of the three occupied fcc sublattices individually in order to optimize the thermoelectric properties. The only drawback is the relatively high thermal conductivity, which is often as high as 10 W/mK. A maximal ZT value of 1.4 at 700 K was reported for the compound $(\text{Zr}_{0.5}\text{Hf}_{0.5})_{0.5}\text{Ti}_{0.5}\text{NiSn}_{0.998}\text{Sb}_{0.002}$ [S. Sakurada and N. Shutoh, *Appl. Phys. Lett.* 86, 082105 (2005)]. For an n-type TiCoSb-based material, the highest ZT value reported so far, is 0.7 at 900 K for $\text{Ti}_{0.6}\text{Hf}_{0.4}\text{Co}_{0.87}\text{Ni}_{0.13}\text{Sb}$ with a power factor of $23.4 \mu\text{Wcm}^{-1}\text{K}^2$ [S. Bhattacharya, et al., *Appl. Phys. Lett.* 77, 2476 (2000)]. A further important issue is the preparation of single crystals in order to investigate the intrinsic properties. This is the basis for further enhancement of the thermoelectric performance of Half-Heusler compounds. Indeed, $\text{Zr}_{0.5}\text{Hf}_{0.5}\text{NiSn}$ single crystals show a high intrinsic ZT value of 0.4 at 350 K [S. Ouardi, et al., *Appl. Phys. Lett.* 99, 152112 (2011)] which possibly leads to a $ZT > 1$ at 800 K. In general we can reproduce the high ZT values of the Japanese groups. Jointly with Bosch we have found that the origin of the high ZT in Heusler compounds is phase separation and spinodal decomposition which reduce the thermoconductivity [DE 10 2010 029 968].

Multifunctional topological insulators

Many excellent thermoelectric materials are also topological insulators (TI). One of the first TI-systems was the quantum well structure of CdTe/HgTe/CdTe. With the introduction given above it is obvious that Heusler compounds are ideal multifunctional topological insulators. Around 50 Heusler compounds show a band inversion, similar to that reported for HgTe, where the quantum spin Hall effect was experimentally observed [M. König et al., *Science*, 318, 766 (2007)]. Similar like in HgTe the topological state in these zero-gap semiconductors can be created by

lich, dass Heusler-Verbindungen ebenfalls ideale multifunktionale topologische Isolatoren sein können [siehe Reporte *A Recipe for Topological Insulators* (Seite 228), und *Electronic Structure of Heusler Compounds with Cl_b Structure and "Zero Band Gap"* (Seite 232)]. Ungefähr 50 Heusler-Verbindungen zeigen eine Bandinversion ähnlich wie in HgTe, in dem der Quantenspin-Hall-Effekt experimentell beobachtet wurde [M. König et al., *Science*, 318, 766 (2007)]. In diesen „Zero-Gap-Halbleiter“ genannten Verbindungen kann der topologische Zustand entweder durch eine strukturelle Verzerrung oder durch den Aufbau einer Quantentopfstruktur erzeugt werden. Vieler dieser ternären Zero-Gap-Halbleiter enthalten Seltenerd-elemente mit stark korrelierten f-Elektronen, was wiederum zu weiteren Eigenschaften wie Supraleitung (z. B. in LaPtBi), Magnetismus [GdPtBi] und Schweres-Fermion-Verhalten (YbPtBi) führt [siehe Beitrag *A Recipe for Topological Insulators* (Seite 228)].

Spinelektronik

Spinelektronik ist eine der neuen Disziplinen, die es schaffen können, den wachsenden Bereich der Informationstechnologie zu revolutionieren. Die Forschung an Heusler-Verbindungen für Spintronik-Anwendungen wurde durch unsere Entdeckung eines großen negativen Magnetwiderstands (magneto-resistiver Effekt = MR-Effekt) in der quaternären Heusler-Verbindung $\text{Co}_2\text{Cr}_{0,6}\text{Fe}_{0,4}\text{Al}$ (CCFA) begründet [T. Block, et al., *J. Solid State Chem.* 176, 646 (2003); DE10108760A1, H01L43/08, WO/2002/069356, EP2002722119, CH02805360.5, JP2002568388, US10469098, KR1020037011101]. Durch ein gezieltes Design haben wir eine Heusler-Verbindung mit hoher Spinpolarisation hergestellt. Kurz nach der Veröffentlichung unserer Ergebnisse hat die Gruppe um Inomata, Tohoku Universität, diese Verbindung in Tunnelkontakten eingesetzt und zum erstenmal einen großen Tunnelmagnetwiderstand (tunneling magnetoresistance TMR) von 26.5% bei 5 K (16% bei Raumtemperatur) gefunden, mit CCFA als Elektrode [K. Inomata, S. Okamura, R. Goto, and N. Yezuka, *Jpn. J. Appl. Phys.* 42, L419 (2003)]. Die Verwendung von Heusler-Verbindungen in TMR-Bauteilen führte in den folgenden Jahren zu einer dramatischen Erhöhung des TMR-Effekts und gleichzeitig zu unserer intensiven Zusammenarbeit mit der Tohoku Universität (Japan) und zahlreichen

Unternehmen. Mit Co_2FeSi haben wir die Heusler-Verbindung mit der höchsten Curie-Temperatur (1100 K) und dem höchsten magnetischen Moment von $5.97 \mu_B$ [S. Wurmehl, et al., *J. Appl. Phys.* 99, 08J103 (2006)] entdeckt. Zusätzlich wurde die Temperaturabhängigkeit des Magnetwiderstands durch die Justierung der Fermienergie in der Mitte der Bandlücke von $\text{Co}_2\text{FeSi}_{0,5}\text{Al}_{0,5}$ [G. H. Fecher and C. Felser, *J. Phys. D: Appl. Phys.* 40, 1582 (2007)] oder $\text{Co}_2\text{Mn}_{0,5}\text{Fe}_{0,5}\text{Al}_{0,5}$ verbessert [B. Balke, et al., *Phys. Rev. B* 74, 104405 (2006)]. Ein Überschuss von Mangan in Co_2MnSi in epitaktischen Tunnelkontakten führte zu einem TMR Wert von mehr als 2000 % bei 4.2 K und ~400 % bei Raumtemperatur [M. Yamamoto, private Mitteilung].

Für die kommende Generation von Festplatten-Leseköpfen wird ein Wechsel bei der Elektroden-Geometrie stattfinden: weg von der „cip“-Geometrie (Strom fließt in Richtung der Magnetisierung der Elektrode) zur „current-perpendicular-to-plane (cpp)“ Geometrie, bei der der Strom senkrecht zu Magnetisierung fließt. Rekorde halten auch hier Funktionseinheiten mit Heusler-Verbindungen [K. Sakamoto, et al., US Patent, 2010/015746535]. Ein neues Konzept für einen cpp-GMR-Kontakt ausschließlich auf der Basis von Heusler-Verbindungen ist erst kürzlich von uns entwickelt und patentiert worden: halbmetallische Ferromagnete, die mit nichtmagnetischen, halbleitenden quaternären Heusler-Verbindungen kombiniert werden, haben garantiert halbmetallische Grenzflächen. Wegen der Durchstimmbbarkeit von Heusler-Verbindungen ist es sogar möglich, durch den Austausch von nur einem Element eine Kombination eines halbmetallischen Ferromagneten mit einer halbleitenden Verbindung zu wählen. Als Beispiele können hier Co_2MnAl und CoMnVAl genannt werden [S. Chadov, et al., *Phys. Rev. Lett.* 107, 047202 (2011)].

Spin transfer torque

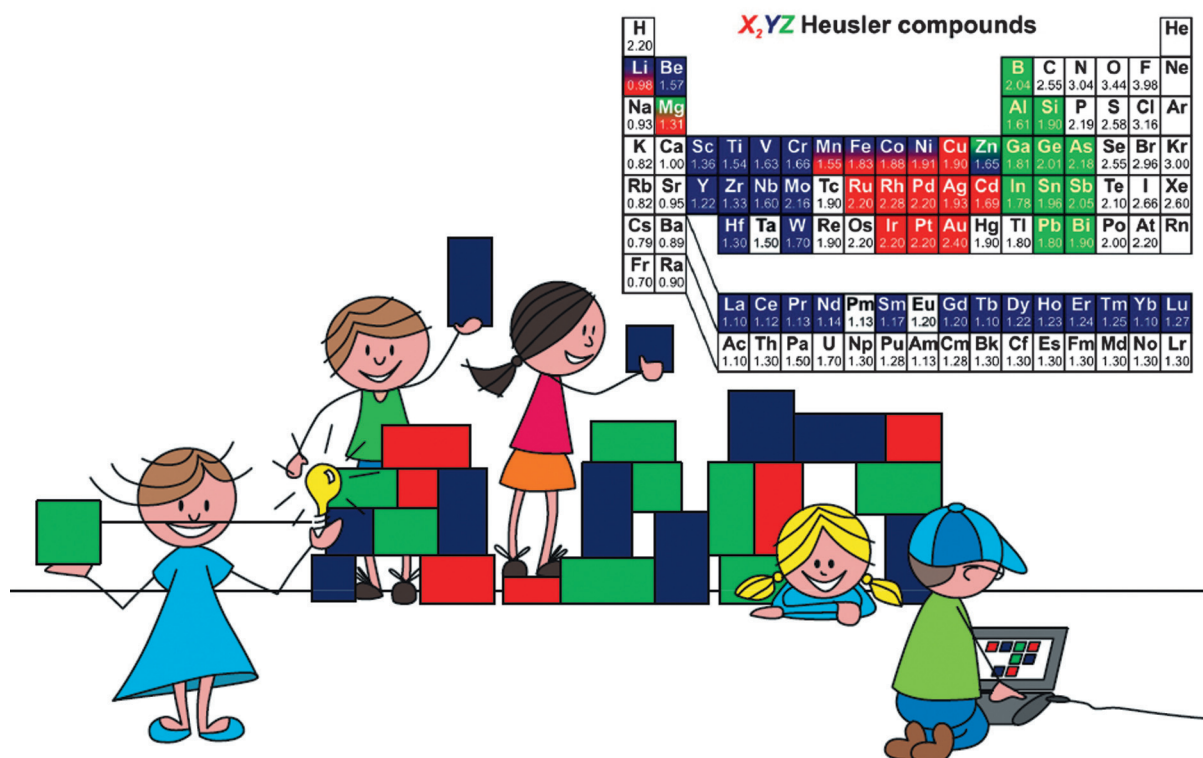
Jüngste Entwicklungen von praktikablen Spintronik-Bauelementen basieren auf Spin Transfer Torque (STT). Hier wird die Magnetisierungsrichtung der Elektrode nicht durch ein magnetisches Feld geändert, sondern durch einen geringen elektrischen Strom. Ziel ist es, die sogenannten DRAM Speicher im Computer durch energiesparende magnetische RAM zu ersetzen und das mit Abmessungen der individuellen Bits unter

applying strain or by designing an appropriate quantum well structure. Many of these ternary zero-gap semiconductors contain a rare-earth element with strongly correlated *f* electrons, yielding additional properties ranging from superconductivity (e.g. LaPtBi) to magnetism (e.g. GdPtBi) and Heavy Fermion behavior (e.g. YbPtBi). For details see report *A Recipe for Topological Insulators* (page 228).

Spintronics

Spintronics is one of the emerging disciplines that continue to revolutionize the thriving field of information technology. The research on Heusler compounds for spintronic applications was stimulated by our discovery of a large negative magnetoresistance (MR) at RT in the quaternary Heusler compound $\text{Co}_2\text{Cr}_{0.6}\text{Fe}_{0.4}\text{Al}$ (CCFA) [T. Block, et al., *J. Solid State Chem.* 176, 646 (2003); DE10108760A1, H01L43/08, WO/2002/069356, EP2002722119, CH02805360.5, JP2002568388, US10469098, KR1020037011101], which demonstrated the tunability of the spin density of states at the Fermi level by substituting constituent elements. Shortly after that, the first tunneling magnetoresistance (TMR) effect using a B2 sputtered CCFA electrode was reported to be 26.5% at 5 K (16% at RT) by Inomata et al. [K. Inomata, S.

Okamura, R. Goto, and N. Yezuka, *Jpn. J. Appl. Phys.* 42, L419 (2003)]. The incorporation of Heusler compounds into TMR devices has led to a dramatic increase in the TMR ratio in the following years and to an intense collaboration with Tohoku University and several companies. With Co_2FeSi we have found the half metallic Heusler compound with the highest magnetic moment of $5.97 \mu_B$ and Curie temperature of 1100 K [S. Wurmehl, et al., *J. Appl. Phys.* 99, 08J103 (2006)]. Additionally the temperature dependence of the TMR was improved by adjusting the Fermi energy in the middle of the gap using $\text{Co}_2\text{FeSi}_{0.5}\text{Al}_{0.5}$ [G. H. Fecher and C. Felser, *J. Phys. D: Appl. Phys.* 40, 1582 (2007)] or $\text{Co}_2\text{Mn}_{0.5}\text{Fe}_{0.5}\text{Si}$ [B. Balke, et al., *Phys. Rev. B* 74, 104405 (2006)]. The use of manganese excess in Co_2MnSi in fully epitaxial magnetic tunnel junctions (MTJ) resulted in high TMR ratios of more than 2000% at 4.2 K and ~400% at RT [M. Yamamoto, unpublished results]. From the commercial side, Heusler compounds are mainly investigated in the context of magnetic recording [K. Kodama, et al., *J. Appl. Phys.* 105, 07E905 (2009), T. M. Nakatani, et al., *Appl. Phys. Lett.* 96, 212501 (2010), T. Mizuno, et al., *IEEE Trans. Magn.* 44, 3584 (2008), M. J. Carey, J. R. Childress, and S. Maat, US Patent, 2008/0112095]. Read heads utilizing the current-in-plane (cip) geometry have



10 nm. Dünne Filme mit senkrechter magnetischer Anisotropie (PMA), d. h. mit einer Magnetisierungsachse senkrecht zur Filmoberfläche, bieten sich als Spintronik-Materialien an, um die superparamagnetische Grenze zu überwinden und die thermische Stabilität der Bits zu vergrößern. Auch hier können wir der Spintronik-Gemeinschaft Lösungen anbieten. Stabile Heusler-Verbindungen mit uniaxialer magnetischer Anisotropie wie Mn_3Ga , die die notwendige niedrige Gilbert Dämpfung, hohe Spinpolarisation, niedrige Sättigungsmagnetisierung und hohe Curietemperatur besitzen, können in der Klasse der tetragonalen Heusler-Verbindungen gefunden werden. Nach unseren ersten Veröffentlichungen [B. Balke, et al., Appl. Phys. Lett. 90, 152504 (2007), J. Winterlik, et al., Phys. Rev. B 77, 054406 (2008)] haben ver-

schiedene Gruppen die ausgezeichneten Eigenschaften von Mn_3Ga und verwandten Verbindungen für Spin-Transfer-Torque-Anwendungen bestätigt [F. Wu, et al., Appl. Phys. Lett. 94, 122503 (2009)]. Weitere tetragonale Mn_2YZ Verbindungen ($Y=Mn, Fe, Co, Rh, Pt; Z=Ga, Sn$) sind inzwischen in unserem virtuellen Labor als potenzielle Materialien für STT-Anwendungen [siehe Beitrag *Tetragonal Heusler Compounds for Spintronics* (Seite 217)] identifiziert worden. Ein Nebeneffekt unserer Forschung an tetragonalen Heusler-Verbindungen ist, dass jetzt Firmen, die FePt für Speichermedien verwenden, und Gruppen, die an Seltenerd-freie Hartmagneten arbeiten, ebenfalls an der Klasse der „durchstimmbaren“ tetragonalen Heusler-Materialien interessiert sind.

recently been replaced by heads based on the current-perpendicular-to-plane (cpp) tunneling MR effect [K. Sakamoto, et al., US Patent, 2010/015746535]. A new design scheme for an all Heusler cpp-GMR junction was invented and patented by us recently; half-metallic ferromagnets can be combined with nonmagnetic, semiconducting quaternary Heusler materials that can be derived from the half-metal by exchanging only one element, for instance Co_2MnAl and CoMnVAI [S. Chadov, et al., Phys. Rev. Lett. 107, 047202 (2011)]. Thus it becomes possible to engineer the interfaces and create non-destructive interfaces, which preserve the half-metallicity.

Spin transfer torque

Recent development of practical spintronic devices is based on Spin Transfer Torque (STT), which provides an ultra-low-power switching (writing) solution and allows for the scaling of the individual bit cell size below the 10 nm industry node. Thin films with perpendicular magnetic anisotropy (PMA), i.e. with the easy magnetization axis pointing perpendicular to the film surface, are strongly desired for spintronics applications to overcome the superparamagnetic limit and enhance the thermal stabil-

ity of the devices. Also for this problem we could offer a solution to the spintronics community. Stable Heusler compounds with uniaxial magnetic anisotropy such as Mn_3Ga are extremely promising as the necessary low damping, high spin polarisation, low saturation magnetisation and high Curie temperature can be simultaneously found within this broad class of materials. After our first publications [B. Balke, et al., Appl. Phys. Lett. 90, 152504 (2007), J. Winterlik, et al., Phys. Rev. B 77, 054406 (2008)] several groups could prove the fantastic performance of Mn_3Ga and related compounds for spin transfer torque applications [F. Wu, et al., Appl. Phys. Lett. 94, 122503 (2009)]. Further tetragonal Mn_2YZ Heusler compounds ($Y=\text{Mn, Fe, Co, Rh, Pt}$; $Z=\text{Ga, Sn}$) were identified via our virtual laboratory approach as potential materials for STT applications [see report *Tetragonal Heusler Compounds for Spintronics* (page 217)]. A side effect of our search for new tetragonal Heusler compounds is that now also companies working on media based on FePt and groups working on rare earth free hard magnets, shape memory alloys and magneto-calorics are strongly interested in the enormous class of tunable tetragonal Heusler compounds.

HAXPES: Spin Polarization, Linear and Circular Magnetic Dichroism in Angle-Resolved Hard X-ray PhotoElectron Spectroscopy

Gerhard H. Fecher and Claudia Felser

Heusler compounds have attracted scientific and technological interest and are now widely used as materials for magneto-electronic devices [1]. One major technology where Heusler compounds are used is on tunneling magneto resistive (TMR) junctions. To develop high performance spintronic devices, it is essential to clarify the electronic structures of these films and compare them to bulk materials.

Photoelectron spectroscopy is one of the best suited techniques to study the occupied electronic structure of materials. Low kinetic energies, however, result in a small electron mean free path of only 4 Å–5 Å at kinetic energies of about 100 eV. That is, the escape depth of the electrons is less than one cubic cell of Heusler compounds with lattice parameters of typically 5 Å–6 Å. Mainly the surface will contribute to the intensity if using VUV light (about 10 eV–50 eV) or soft x-rays (below 1 keV) for excitation. In the contemporary x-ray photoelectron spectroscopy (XPS) one uses photons of medium energies for excitation. The use of Mg K_{α} or Al K_{α} sources results for typical Heusler compounds in an escape depth of about 19 Å–25 Å at kinetic energies of 1.2 keV or 1.4 keV. The situation improves much at higher energies. In hard XPS (HAXPES) with excitation energies of about 8 keV high bulk sensitivity is reached with an escape depth being larger than 115 Å (corresponding to 20 cubic cells of a Heusler compound). High energy photoemission was already used by Siegbahn and co-workers when exploring electron spectroscopy for chemical analysis (ESCA) [2]. Lindau et al. [3] demonstrated in 1974 the possibility of synchrotron radiation based high energy photoemission with energies up to 8 keV, however, no further attention was devoted to such experiments for many years. Nowadays, high energy excitation and analysis of the electrons become easily feasible due to the development of high intense sources (insertion devices at synchrotron facilities) and multichannel electron detection. Thus, high energy photoelectron spectroscopy was recently introduced by several groups as a bulk sensitive probe of the electronic structure in complex materials.

Hard x-ray photoelectron spectroscopy (HAXPES) is a powerful method to probe both chemical states and electronic structure of bulk materials [4] and buried layers in a non-destructive way [5]. The combination of HAXPES with polarized radiation for excitation significantly extends its applicability. The use of linearly s and p polarized light in HAXPES enables the analysis of the symmetry of bulk electronic states [6]. In the present study the valence band electronic structure of NiMnSb bulk material was investigated by means of HAXPES and linear dichroism. The $2p$ core level of a thin exchange biased thin film of Co_2FeAl as used in TMR devices was studied by means of HAXPES combined with circular magnetic dichroism [7].

The first spin resolved HAXPES (SPIN HAXPES) experiments world-wide have been performed by our group at SPring-8 (Hyogo, Japan) [8] and at PETRA III (Hamburg, Germany) [9] employing different types of spin detectors, that are low energy scattering SPLEED detectors and high energy scattering Mott-detectors, respectively.

The “*dichroic*” HAXPES experiments were performed at BL47XU of SPring-8 (Hyogo, Japan) using about 8 keV linearly and circularly polarized photons for excitation. The photon energy was fixed at 7.9392 keV using a Si(111) double crystal monochromator (DCM) and the 444 reflection of reflection of a Si channel-cut post monochromator. Horizontal (p) polarization was obtained directly from the undulator without any additional polarization optics. An in-vacuum phase retarder based on a 300- μm -thick diamond crystal was used to produce vertical, linearly s -polarized light or circularly $\sigma+$ or $\sigma-$ polarized light, all with a degree of polarization above 90%. Grazing incidence ($\alpha = 88^\circ$) – normal emission ($\theta = 2^\circ$) geometry was used that ensures that the polarization vector was nearly parallel (p) or perpendicular (s) to the surface normal or that the polarization vector σ coincides with the magnetization. The photoemitted electrons were analyzed for their kinetic energy and detected by means of a hemispherical analyzer (Scienta R4000–12 kV). The valence band spectra were taken with a total energy resolution of 140 meV or

240 meV as verified by spectra of the Gold Fermi energy. The sample temperature was set to 20 K in all measurements. For further details of the HAXPES experiment see References [10,11,12,13]. First spin-resolved HAXPES experiments at BL47-XU of SPring-8 have been performed using a combination of a Scienta R-4000-10keV hemispherical analyzer with a spin detector based on spin polarized low energy electron diffraction (SP)LEED at a W(100) surface. For the spin resolved measurements with the SPLEED detector, the photon energy was set to 5.95 keV because of a higher photoelectron intensity expected from the increase of ionization cross section at lower energies [8].

Figure 1 compares the valence band spectra and calculated electronic structure of NiMnSb. The density of states exhibits a typical 4-peak structure in the energy range of the d states as well as the split-off s -band with a_1 symmetry. These structures are clearly resolved in the spectra. The sum of the polarization-resolved spectra corresponds to a spectrum with unpolarized photons. The width of the d -

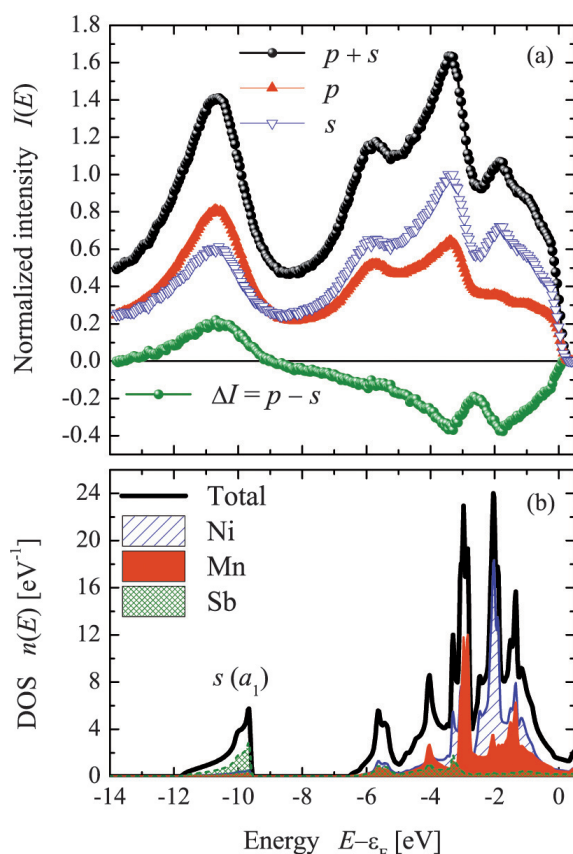


Fig. 1: Electronic structure and polarization-dependent photoelectron spectra of NiMnSb. (a) Spectra obtained with s and p polarized light together with the sum and difference and (b) total and partial density of states (DOS).

part of the density of states (0 ... 5 eV) corresponds to the width of the measured spectra. The spectrum exhibits a rather high intensity in the a_1 -part below -7 eV that is caused by the higher cross section for s -states compared to d -states at high excitation energy. The intensity of the d -states is governed by the states localized at the Ni atoms. It is evident that striking differences appear in the spectra if the polarization is changed from p to s . The spectra indicate that the a_1 states have a higher intensity for p polarization and the s polarization results in a higher intensity in the energy range of the d -states. In particular, the intensity of the Ni $3d$ states at -2 eV is enhanced and the structure of the density of states becomes better resolved under illumination with s polarized photons. These observations show that the symmetry of the states can be explored using linearly polarized photons [6].

Figure 2 shows the Fe $2p$ and the “shallow” core levels of a deeply buried Co_2FeAl film underneath 10 nm of MnIr. The differences in the spectra taken with opposite helicity of the photons at a fixed direction of magnetization are very pronounced. The spin-orbit splitting of the Fe $2p$ states is clearly resolved, as expected. If going from $2p_{3/2}$ to $2p_{1/2}$, the dichroism changes its sign across the $2p$ spectra in the series $-++-$ what is typical for a Zeemann-type m_j sub-level ordering. Details of the MCDAD reveal, however, that the situation is more complicated. For such complex multilayer structures the situation becomes complicated in the way that the signals from all the elements contained in the system are detected. One still notices strong signals from the buried elements even though the ferromagnetic Co_2FeAl layer lies underneath the antiferromagnetic IrMn layer. As expected no MCDAD is observed for the Ir and Mn states. A non-vanishing asymmetry is clearly observed only for Co and Fe signals that are just the ones being responsible for the ferromagnetic properties of the system. The asymmetry of 50% in the Fe $3p$ signal is huge. At the Co $3p$ it is well detected even though the direct spectra overlap with Ir states. A comparison to results from CoFe thin films is found in Reference [7].

First spin-resolved HAXPES experiments at undulator beamline P09 of PETRA III (Hamburg, Germany) have been performed by a combination of a SPECS Phoibos 225 HV hemispherical analyzer with a combined delayline detector and four channel micro-Mott spin detector [9]. The delay-

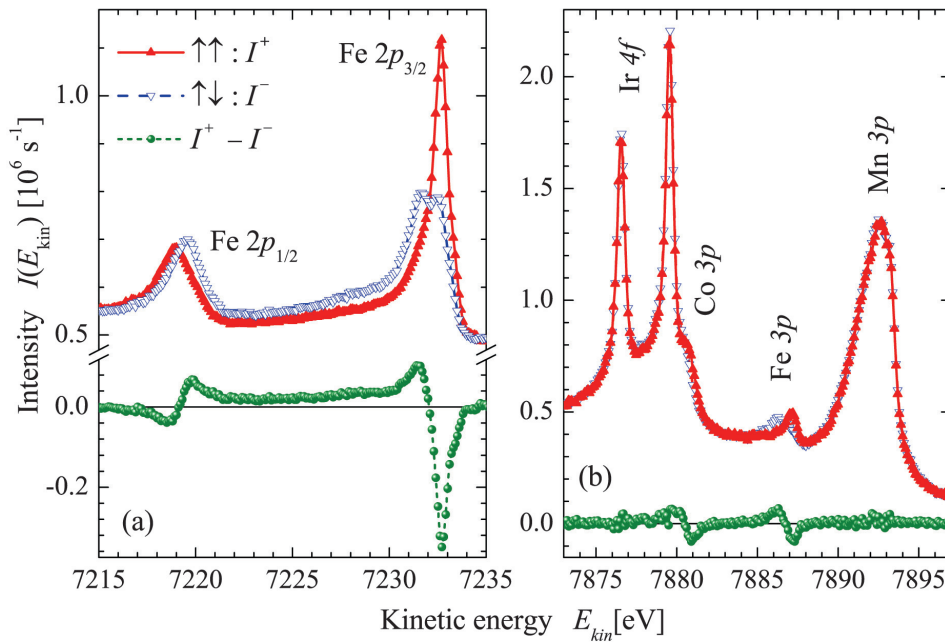


Fig. 2: High kinetic energy core level spectra and MCDAD from Co_2FeAl underneath a 10 nm thick IrMn film. (a) Fe 2p core level; (b): shallow core levels.

line detector allows parallel detection of angular or spatial distributions of the photoemitted electrons. The micro-Mott spin detector is based on polarized electron scattering at a thin Au foil at 20 keV energy and can be operated in parallel to the delayline detector. The spin-resolved measurements were conducted with 100 mA ring current using a focused beam with $0.2 \times 0.4 \text{ mm}^2$ spot size. The photon energy was set to 4.5 keV using a Si(111) DCM, the total energy resolution was 500 meV.

The spin-resolved HAXPES data obtained from a buried CoFe layer are shown in Figure 3. The integral Fe 2p spectrum (dotted line) taken with all four channels of the micro-Mott spin detector has an intensity of about $5 \times 10^4 \text{ s}^{-1}$. The asymmetry is due to the exchange splitting and changes its sign when the sample magnetization is rotated by 180° . A spin polarization of 10% is determined at the Fe $2p_{3/2}$ core level. The majority component of the Fe $2p_{3/2}$ and Fe $2p_{1/2}$ states has a higher binding energy as the minority one. The qualitative behavior of sign change is consistent with the magnetic dichroism data. Also, the results are consistent with magnetic circular dichroism experiments [13,14], and spin-resolved data [15] of ferromagnetic Fe surfaces. The experiment clearly demonstrates that spin-resolved core level HAXPES using a Mott detection system is feasible and may be effectively

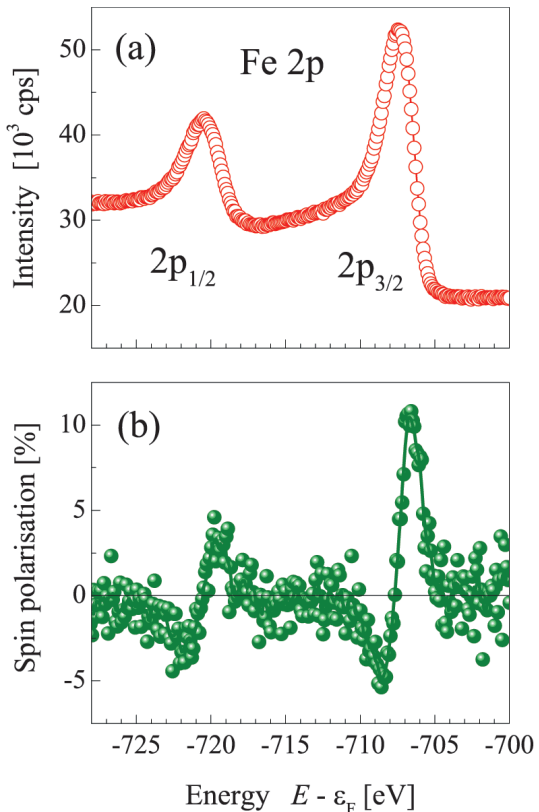


Fig. 3: Fe 2p photoelectron spectra (a) taken with the 4-channel micro-Mott spin detector and resulting spin polarization (b). The solid line is a guide to the eye.

used to probe buried magnetic structures and can be extended to valence band spectroscopy in near future.

Overall, the high bulk sensitivity of HAXPES combined with linearly and circularly polarized photons will have a major impact on the study of the magnetic phenomena of magnetic materials. It will allow an element-specific study of the magnetism of buried layers and make feasible the investigation of the properties of magnetic layers not only at the surface but also at buried interfaces. The results obtained with circularly polarized photons confirm the possibility to distinguish between localized or itinerant character of the magnetic moments in complex compounds. The symmetry of valence states can be determined when using linearly polarized photons. Finally, the further development of SPIN-HAXPES will allow to disentangle the role of the spin polarization at the Fermi energy of halfmetallic ferromagnets.

We thank all members of the group, the “*photoemission crew*”, and especially the staff of SPring-8 and PETRA III for their help with and realization of all those demanding experiments. This research is financially supported by Deutsche Forschungsgemeinschaft (DFG) (project no. TP 1.3-A of Research Unit FOR 1464 ASPIMATT) and DfG-JST (project no. FE633/6-1). The HAXPES experiments at BL47XU of SPring-8 (Hyogo, Japan) were performed with the approval of the Japan Synchrotron Radiation Research Institute (JASRI) (long-term Proposal 2008B0017). Experiments at PETRA-III are funded by the Federal Ministry of Education and Research (BMBF) (contracts no.: 05KS7UM1, 05K10UMA)

References

- [1] *C. Felser, G. H. Fecher, B. Balke*, *Angew. Chem. Int. Ed.* **46** (2007) 668.
- [2] *C. Nordling, E. Sokolowski, K. Siegbahn*, *Phys. Rev.* **105** (1957) 1676.
- [3] *I. Lindau, P. Pianetta, S. Doniach, and W. E. Spicer*, *Nature* **250** (1974) 214.
- [4] *S. Ouardi, G. H. Fecher, B. Balke, A. Beleanu, X. Kozina, G. Stryganyuk, C. Felser, W. Klöß, H. Schrader, F. Bernardi, J. Morais, and E. Ikenaga*, *Phys. Rev B* **84** (2011) 155122.
- [5] *G. H. Fecher, B. Balke, A. Gloskovskii, S. Ouardi, C. Felser, T. Ishikawa, M. Yamamoto, Y. Yamashita, H. Yoshikawa, S. Ueda, K. Kobayashi*, *Appl. Phys. Lett.* **92** (2008) 193513.
- [6] *S. Ouardi, G. H. Fecher, X. Kozina, G. Stryganyuk, B. Balke, C. Felser, E. Ikenaga, T. Sugiyama, N. Kawamura, M. Suzuki, K. Kobayashi*, *Phys. Rev. Lett.* **107** (2011) 036402.]
- [7] *X. Kozina, G. H. Fecher, G. Stryganyuk, S. Ouardi, B. Balke, C. Felser, G. Schönhense, E. Ikenaga, T. Sugiyama, N. Kawamura, M. Suzuki, T. Taira, T. Uemura, M. Yamamoto, H. Sukegawa, W. Wang, K. Inomata, K. Kobayashi*, *Phys. Rev. B* **84** (2011) 054449]
- [8] *G. Stryganyuk, X. Kozina, G. H. Fecher, S. Ouardi, S. Chadov, C. Felser, G. Schönhense, A. Oelsner, P. Bernhard, E. Ikenaga, T. Sugiyama, H. Sukegawa, Z. Wen, K. Inomata, K. Kobayashi*, *Jpn. J. Appl. Phys.* **51** (2012) 016602.
- [9] *A. Gloskovskii, G. Stryganyuk, G. H. Fecher, C. Felser, S. Thiess, H. Schulz-Ritter, W. Drube, G. Berner, M. Sing, R. Claessen, and M. Yamamoto*, *J. Electron Spectrosc. Relat. Phenom.* **185** (2012) 47.
- [10] *S. Ouardi, C. Shekhar, G. H. Fecher, X. Kozina, G. Stryganyuk, C. Felser, S. Ueda, and K. Kobayashi*, *Appl. Phys. Lett.* **98** (2011) 211901.
- [11] *C. Shekhar, S. Ouardi, G. H. Fecher, A. K. Nayak, C. Felser, and E. Ikenaga*, *Appl. Phys. Lett.* **100** (2012) 252109.
- [12] *S. Ouardi, G. H. Fecher, X. Kozina, G. Stryganyuk, B. Balke, C. Felser, E. Ikenaga, T. Sugiyama, N. Kawamura, M. Suzuki, and K. Kobayashi*, *Phys. Rev. Lett.* **107** (2011) 036402.
- [13] *X. Kozina, G. H. Fecher, G. Stryganyuk, S. Ouardi, B. Balke, C. Felser, G. Schönhense, E. Ikenaga, T. Sugiyama, N. Kawamura, M. Suzuki, T. Taira, T. Uemura, M. Yamamoto, H. Sukegawa, W. Wang, K. Inomata, and K. Kobayashi*, *Phys. Rev. B* **84** (2011) 054449.
- [14] *L. Baumgarten, C. M. Schneider, H. Petersen, F. Schäfers, J. Kirschner*, *Phys. Rev. Lett.* **65** (1990) 492.
- [15] *D. G. van Campen, R. J. Pouliot, L. E. Klebanoff*, *Phys. Rev. B* **48** (1993) 17533.

Magnetic Dichroism in Angle-Resolved Hard X-ray Photoemission from Magnetic Thin Films

Carlos E. Viol Barbosa, Daniel Ebke, Siham Ouardi, Eiji Ikenaga¹, Gerhard H. Fecher, and Claudia Felser

Here, we report on the investigation of magnetic dichroism in angular-resolved photoemission (MCDAD) from in-plane magnetized buried thin films. The high bulk sensitivity of hard X-ray photoelectron spectroscopy (HAXPES) in combination with circularly polarized radiation enables the investigation of the magnetic properties of buried layers. By using an optimized electrostatic wide-angle lens setup, we were able to measure the angular distribution of high-energy photoelectrons in a range of about 60° . The experiments were performed on exchange-biased magnetic layers covered by thin oxide films. More specifically, we investigate the angular distribution in photoemission from a ferromagnetic Co_2FeAl layer grown on a MnIr exchange-bias layer; the structure is buried underneath a MgO layer as usually used in tunneling magnetoresistance (TMR) devices. A pronounced magnetic dichroism is found at the Co and Fe 2p states for all photoemission angles.

Magnetic circular dichroism (MCD) in photoabsorption and photoemission has become a very powerful tool for the element-specific investigation of the magnetic properties of alloys and compounds. Thus far, such studies have been mainly carried out using soft X-rays, resulting in a rather surface sensitive technique due to the low electron mean free path of the resulting low energy electrons. The application of hard X-rays results in the emission of electrons with high kinetic energies and thus, it increases the probing depth. The bulk sensitivity of this technique was recently proved and for $h\nu > 8$ keV, the bulk spectral weight was found to reach more than 95%. Hard X-ray photoelectron spectroscopy (HAXPES) has been found to be a well adaptable non-destructive technique for the analysis of chemical and electronic states [1]. It was recently shown that HAXPES can be combined easily with variable photon polarization when using phase retarders [2]. In combination with excitation by circularly polarized X-rays [3], this method will serve as a unique tool for the investigation of the electronic and magnetic structure of deeply buried layers and interfaces.

The HAXPES experiments with polarized hard X-rays (7.940 keV) were performed at beamline BL47XU of SPring-8. The energy and angular distribution of the photoemitted electrons was analyzed using a high energy hemispherical analyzer (Scienta R4000–12 kV). For angular resolved measurements, a special wide-acceptance angle objective lens was placed in front of the Scienta electron optics [4]. By this lens, the effective acceptance angle is increased to about 60° with an angular resolution of better than 1° .

The overall energy resolution was set to 250 or 350 meV, the latter was used for an improved signal to noise ratio while taking the complete 2D angular/energy distributions. The angle between the electron spectrometer and the photon propagation was fixed at 90° . The angle of incidence was set to $\alpha = 89^\circ$ in order to ensure that the polarization vector of the circularly polarized photons is nearly parallel (σ^-) or antiparallel (σ^+) to the in-plane magnetization M . The sign of the magnetization was varied by mounting samples with opposite directions of magnetization (M^+ , M^-). This allows probing the dichroism by varying both the direction of magnetization and the direction of helicity. The vertical spot size on the sample is $30 \mu\text{m}$, while in horizontal direction, along the entrance slit of the analyzer, the spot was stretched to approximately 7 mm. The polarization of the incident photons was varied using an in-vacuum phase retarder based on a $600\text{-}\mu\text{m}$ -thick diamond crystal with (220) orientation. The direct beam is linearly polarized by $> 99\%$. Using the phase retarder, the degree of circular polarization is set such that $P_c > 0.9$. All measurements were performed at room temperature. For further details of the polarized HAXPES experiment see References [5,3].

DC/RF magnetron sputtering was used for the preparation of “half” tunnel junctions. All films were deposited at room temperature. The layers were deposited on thermally oxidized SiO_2 substrates in the following order: Substrate/Ta(5nm)/Ru(30nm)/MnIr(10nm)/ FM (10nm)/MgO(2nm), were $FM = \text{CoFe}$ or Co_2FeAl . The samples were an-

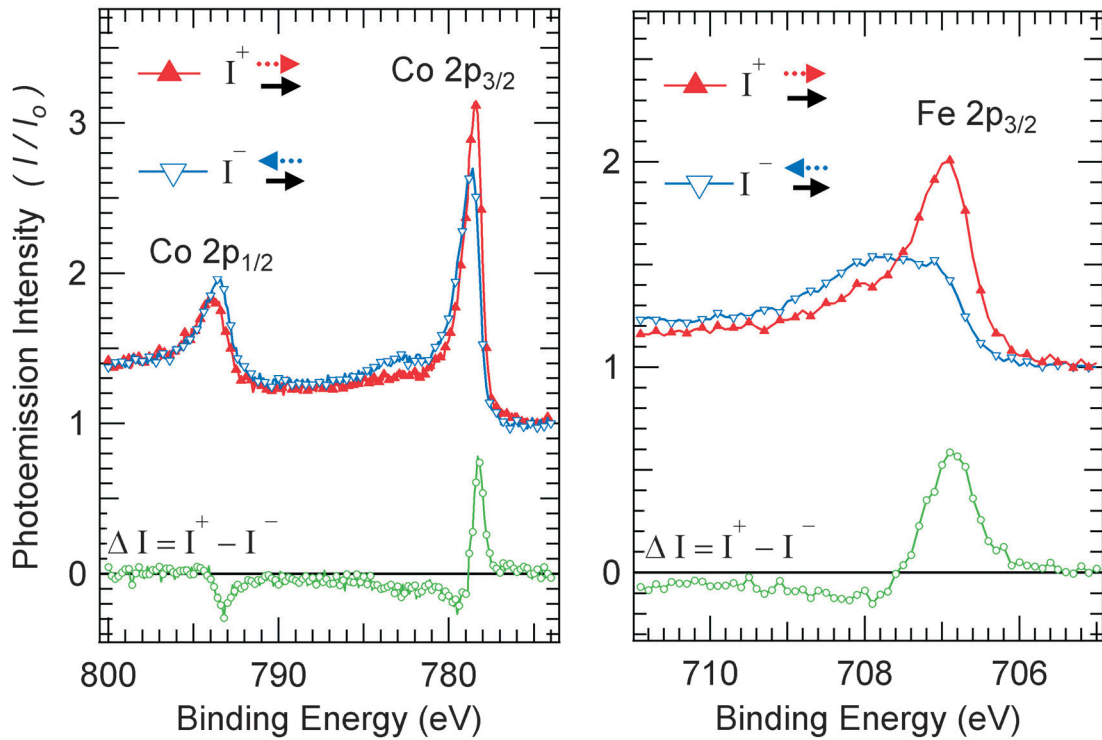


Fig. 1: Polarization-dependent photoelectron spectra of the Co 2p (a) and Fe 2p_{3/2} (b) core-level emission from a 10 nm-thick CoFe film on top of a MnIr exchange-bias layer. I_0 represents the background intensity at the high energy tail. Dotted and solid arrows indicated the X-ray helicity and sample magnetization, respectively. The difference-spectra are shown as dashed lines.

nealed at 275°C for 10 min in vacuum of 5×10^{-2} Pa in a magnetic field of 0.1 T to provide exchange biasing of the ferromagnetic layer film by the anti-ferromagnetic MnIr, in order to keep the CoFe or Co₂FeAl layers magnetized in preset directions.

Figure 1 shows the polarization dependent 2p core level spectra of Co (2p doublet) and Fe (2p_{3/2} only) taken from the exchange biased CoFe film. The spectra were measured in the angular integrated transmission mode. Pronounced differences are observed in the spectra for a fixed direction of magnetization and taken with photons of opposite helicity. The pure difference $\Delta I = I^+ - I^-$ presented in the figure contains all characteristic features of the magnetic dichroism. The dichroism found in the present experiment on CoFe is qualitatively the same as presented in Reference [3].

Figure 2 shows the angular resolved 2p core level spectra of Co and Fe taken from the exchange biased Co₂FeAl film. The spectra were measured in the angular mode, which takes advantage of the new condenser lens system allowing the electrons to be collected from emitted angle from -33° to $+33^\circ$. Each channel detector covers an angle slice

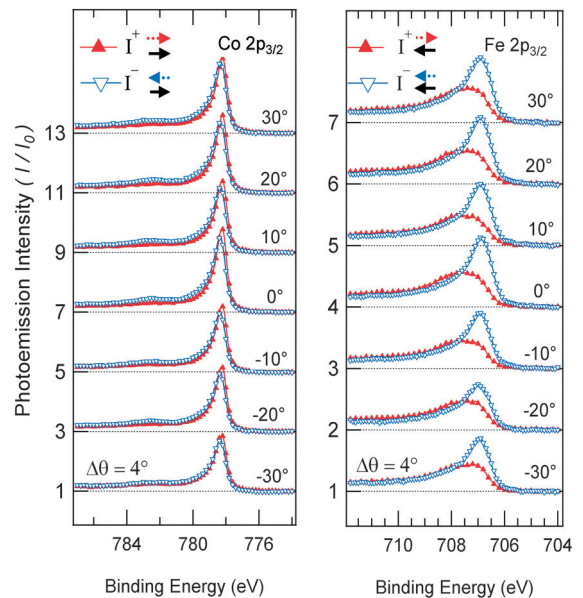


Fig. 2: Angular distribution of polarization dependent photoelectron spectra of the Co(a) and Fe (b) 2p_{3/2} core-level emission from 10nm-thick Co₂FeAl film on top of a MnIr exchange-bias layer. Curves of different photoemission angles are plotted with an offset for clarity.

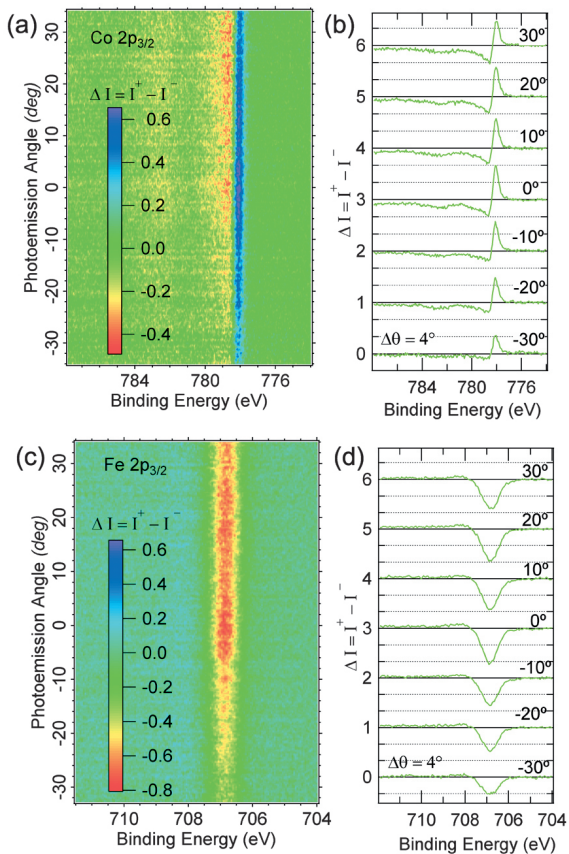


Fig. 3: Angular and energy distribution of the magnetic circular dichroism (ΔI) of the Co $2p_{3/2}$ (a,b) and Fe $2p_{3/2}$ (c,d) core levels in photoemission from a 10 nm-thick Co_2FeAl film. Horizontal line-profiles are shown in the right panel for Co $2p_{3/2}$ (b) and Fe $2p_{3/2}$ (d).

of 0.167° . The spectra shown in the Figure 2 are integrated in slices of $\pm 2^\circ$ (12 channels) about the photoemission direction indicated in the figure. No striking differences can be noticed in the spectral shape. In comparison with the CoFe spectra (see Fig. 1a), the Co $2p_{3/2}$ signal exhibits a shift to lower binding energies and a smaller dichroism. Also, the shape of the Fe 2p emission in Co_2FeAl is similar to CoFe (see Fig. 1b). Small, but important differences that are not directly obvious from the Figures are explained in detail in Reference [3].

Finally, figure 3 shows the complete 2D angular and energy distribution of the MCDAD from the Co 2p and Fe $2p_{3/2}$ core levels taken from the MnIr- Co_2FeAl -MgO multilayer system.

In summary, bulk-sensitive MCDAD-HAXPES was used to image the two dimensional distribution (angle/energy) of electronic states and, in particu-

lar, to study the magnetic response in 2p core level emission from buried ferromagnetic layers. CoFe and Co_2FeAl ferromagnetic films grown on antiferromagnetic MnIr exchange bias layers and buried under MgO layers were analysed. The feasibility to measure the angular and energy distribution of the magnetic dichroism in photoemission by using the new, wide-angle lens setup installed at the HAXPES end-station of beamline BLX47U at SPring-8 is successfully demonstrated.

We thank the SPring-8 staff for their help during the beamtime. This research is financially supported by Deutsche Forschungsgemeinschaft (DFG) (project TP 1.3-A of Research Unit FOR 1464 ASPIMATT). The HAXPES measurements were performed at BL47XU of SPring-8 (Hyogo, Japan) with the approval of the Japan Synchrotron Radiation Research Institute (JASRI) (long-term Proposal 2012B0043).

References

- [1] K. Kobayashi, M. Yabashi, Y. Takata, T. Tokushima, S. Shin, K. Tamasaku, D. Miwa, T. Ishikawa, H. Nohira, T. Hattori, Y. Sugita, O. N. A. Sakai, and S. Zaima, *Appl. Phys. Lett.* **83** (2003) 1005.
- [2] S. Ueda, H. Tanaka, J. Takaobushi, E. Ikenaga, J.-J. Kim, M. Kobata, T. Kawai, H. Osawa, N. Kawamura, M. Suzuki, and K. Kobayashi, *Appl. Phys. Exp.* **1** (2008) 077003.
- [3] X. Kozina, G. H. Fecher, G. Stryganyuk, S. Ouardi, B. Balke, C. Felser, G. Schönhense, E. Ikenaga, T. Sugiyama, N. Kawamura, M. Suzuki, T. Taira, T. Uemura, M. Yamamoto, H. Sukegawa, W. Wang, K. Inomata, and K. Kobayashi, *Phys. Rev. B* **84** (2011) 054449.
- [4] H. Matsuda, H. Daimon, M. Kato, and M. Kudo, *Phys. Rev. E* **71** (2005) 066503.
- [5] S. Ouardi, G. H. Fecher, X. Kozina, G. Stryganyuk, B. Balke, C. Felser, E. Ikenaga, T. Sugiyama, N. Kawamura, M. Suzuki, and K. Kobayashi, *Phys. Rev. Lett.* **107** (2011) 036402.
- [6] X. Kozina, G. H. Fecher, G. Stryganyuk, S. Ouardi, B. Balke, C. Felser, G. Schönhense, E. Ikenaga, T. Sugiyama, N. Kawamura, M. Suzuki, T. Taira, T. Uemura, M. Yamamoto, H. Sukegawa, W. Wang, K. Inomata, and K. Kobayashi, *Phys. Rev. B* **84** (2011) 054449.

¹ Japan Synchrotron Radiation Research Institute, SPring-8, Hyogo, Japan.

A Recipe for Topological Insulators

Lukas Müchler¹, Binghai Yan, Haijun Zhang², Stanislav, Chadov, Frederick Casper¹, Jürgen Kübler³, Gerhard H. Fecher, Xiao-Liang Qi², Shou-Cheng Zhang², and Claudia Felser

Topological insulators are materials with a bulk band gap generated by strong spin–orbit coupling (SOC) and topologically protected metallic surface states, see Figure 1. The TI material is insulating in the bulk, but metallic at the surface and can be identified by a few rules: SOC, an odd number of band inversions (BIs) between the conduction and the valence band by increasing the average nuclear charge, and a sign change of the symmetry of the molecular orbitals.

The recent prediction and experimental verification of the topological insulators (TIs), has generated enormous interest in the field of condensed matter science [1]. To bring this fascinating mathematical concept to life, equations and symmetry considerations have to be translated into bands and bonds. In collaboration with the excellent theory group of Shou-Cheng Zhang from Stanford we formed a successful team to search for new multifunctional TIs. In physics, topology of particles has been studied in the context of high-energy extensions of the standard model using quantum field theory. Charlie Kane and Shou-Chen Zhang have transferred the concept to condensed matter physics, a field in which the corresponding predictions such as Majorana fermions can be easier to be realized as for example in topological superconductors. As inorganic chemists we are experts in understanding materials and their electronic structure. The topological classification of k space developed by theory was mapped onto simple pictures in inorganic chemistry, such as crystal structures, valence elec-

trons, nuclear charges, and the phase of orbitals [2]. Moreover, TIs can be predicted by electronic-structure calculations and even designed by band engineering [3].

In 2006 Bernevig, Hughes and Zhang [4] proposed a general mechanism for finding topological insulators based on band inversion due to spin orbit coupling and in particular predicted that HgTe quantum wells (QWs) are topological insulators. HgTe is a zero-gap semiconductor with an inverted band ordering, the s bands, which are unoccupied in semiconducting CdTe are occupied in HgTe due to the relativistic inner pair effect. The band inversion determines the unique topological feature of HgTe. Since HgTe is a semimetal due to the degenerate p -states at the Fermi energy the energy gap can only open in a quantum well-structure (QW) with CdTe or when the cubic symmetry is broken.

Both HgTe and CdTe have zincblende lattice structure, in which two interpenetrating face-centered-cubic (fcc) lattices shifted along the diagonal of the cubic cell. Half-Heusler compounds with the $C1_b$ structure are ternary relatives of the classical binary semiconductors with three fcc-lattices shifted along the diagonal [5]. The band gaps of these ternary semiconductors can readily be tuned from zero up to 4 eV by simply changing their chemical composition. The diversity of Heusler materials opens wide possibilities for tuning the band gap and setting the desired band inversion by choosing compounds with appropriate hybridization strength (by the lattice parameter) and magni-

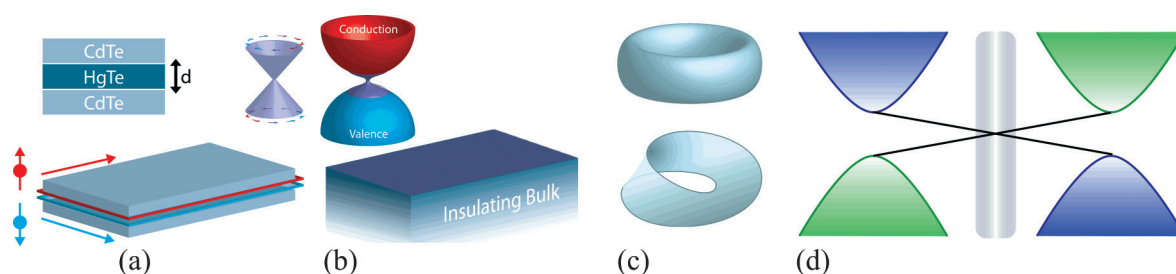


Fig. 1: Schematics of a) a two-dimensional topological insulator (2D TI). Only one of the one-dimensional counter-propagating edge states is shown for each surface. b) 3D TI and schematic band structure with a Dirac cone and c) an example for two topologically distinguished surfaces, a torus and a Möbius stripe and d) illustration of topological states at the interface between a normal insulator (left) and a topological insulator (right). The metallic interface states appear at the crossing point.

tude of spin-orbit coupling (by the atomic charge). Based on first-principle calculations we have demonstrated that around 50 Heusler compounds show band inversion similar to that of HgTe [6]. Since the Heusler class is extremely rich, it provides much wider flexibility in design by tuning the band gap and the SOC. The topological state in these zero-gap semiconductors can be created by applying strain or by designing an appropriate quantum-well structure, similar to the case of HgTe. Many of these ternary zero-gap semiconductors (LnAuPb, LnPdBi, LnPtSb and LnPtBi) contain a rare-earth element Ln, which can realize additional properties ranging from superconductivity (for example LaPtBi) to magnetism (for example GdPtBi) and heavy fermion behavior (for example YbPtBi). These properties can open new research directions in realizing the quantized anomalous Hall effect and topological superconductors.

Trivial and topological semiconductors with inverted band structures can be designed by increasing the average nuclear charge of the ternary compound. ScPtSb exhibits a band structure similar to CdTe, whereas ScPtBi exhibits the same BI as HgTe. The s- and the p-bands are inverted in HgTe and heavy Heusler compounds. If the antibonding s-band becomes bonding, the sign of the eigenvectors changes (change of parity). $C1_b$ Heusler compounds have been grown as thin films in collaborations with Stuart Parkins, IBM, Almaden [Shan Rong et al. to be published]. With hard x-ray photoemission we were able to prove that the experimental electronic structure corresponds to the calculated density of states [7]. The control of the defects, the charge carriers and mobilities will be optimized and quantum well structures will be grown in the near future. Recently some of the $C1_b$ Heusler compounds were predicted to be excellent piezoelectrics. The combination of piezoelectric Heusler compounds and compounds at the borderline between trivial and topological insulators offers the possibility of a switchable device.

Heusler compounds are similar to a stuffed diamond, correspondingly, it should be possible to find the “high Z” equivalent of graphene in a graphite-like structure or in other related structure types with 18 valence electrons and with inverted bands. Indeed the ternary compounds, such as LiAuSe and KHgSb with a honeycomb structure of their Au-Se and Hg-Sb layers feature band inversion very simi-

lar to HgTe which is a strong precondition for existence of the topological surface states [8]. In contrast to graphene, these materials exhibit strong spin-orbit coupling and a small direct band gap at the Γ -point. Since these materials are centrosymmetric, it is straightforward to determine the parity of their wave functions, and hence their topological character. Surprisingly, the compound with strong spin-orbit coupling (KHgSb) is trivial, whereas LiAuSe is found to be a topological insulator. The interplay of mechanisms responsible for the trivial or nontrivial character in these systems, however, differs from the cubic semiconductors studied earlier. The XYZ honeycomb compound can typically be viewed as honeycomb YZ layers with alternating hexagonal layers of X atoms stuffing between neighboring YZ layers. This is similar to the cubic XYZ Heusler compound. The single-layer lattice has only one honeycomb layer in the primitive unit cell, and it exhibits no inversion symmetry. However, the double-layered lattice contains two honeycomb layers with a formula of $X_2Y_2Z_2$, in which two YZ layers are connected by the space inversion at X. The low energy band structure is mainly related to the YZ honeycomb layer, while the X layer affects the coupling between the YZ layers. In particular, it is emphasized that the strong SOC and weak interlayer coupling causes the double band inversion which in turn makes the compound trivial. Since the band-dispersion is small in the double layer compound KHgSb a band inversion occurs at the Γ -point and the A point. An even number of potential Dirac cones leads to a trivial insulator for the same reason why graphene is trivial. LiAuSe with an intermediate SOC and only one band inversion is found to be a topological insulator in the double layer structure.

However, these results have opened an even more detailed investigation of this structure and related structure types as a prototype for layered structures. So-called weak topological insulators were predicted theoretically without naming a certain material or structure type. It is possible to create a YZ layer with an inverted band structure even in KHgSb. Such a layer leads to the formation of a 2D TI, also called a quantum spin Hall (QSH) insulator. By stacking such YZ layers along the z direction, we can obtain weak TIs [9] by retaining an odd number of layers in the primitive cell. Here the odd-layered stacking induces an odd number of band inversions, which is necessary to realize topo-

logical nontrivial band structures. Moreover, it is also possible to tune the intra-layer band inversion and the inter-layer coupling by using different X , Y or Z elements. As a result, we can potentially realize the transition from weak to strong TIs, and even to trivial insulators. The single-layered KHgSb is the most suitable candidate for its large bulk energy gap of 0.24 eV. Its side surface hosts metallic surface states, forming two anisotropic Dirac cones. Though the stacking of even-layered structures leads to trivial insulators, the structures can host a quantum spin Hall layer with a large bulk gap, if an additional single layer exists as a stacking fault in the crystal. Therefore these honeycomb compounds can serve as prototypes to aid in the finding of new weak topological insulators in layered small-gap semiconductors.

The largest band gap due to SOC can be expected in Plutonium compounds, since this is the element with the largest SOC. Since the band gap of TIs results from a forbidden crossing TIs with the largest band gaps can be expected in 5f systems. Recently we theoretically predict a class of topological insulators in 5f elements containing semiconductors, where interaction effects play a dominant role [10]. Especially correlated systems are of great interest for the condensed matter society since these classes of materials allow very often a large change in their properties by an external stimulus. In actinide elements, simple rocksalt compounds formed by Pu and Am lie on the boundary between metals and insulators. We show that interaction drives a quantum phase transition to a topological insulator phase with a single Dirac cone on the surface.

Charlie Kane et al. predicted a topological behavior in bismuth doped with antimony. The most famous 3D TI is Bi_2Se_3 , suggested by Bob Cava, who spends and will spend a significant part of his Humboldt prize time in Dresden. The theoretical model was developed by SC Zhang's team and the first experimental proof was done by angle resolved photo-emission by the Princeton group. A Dirac cones type surface state was observed in single crystals [11]. A kind of misfit between two 3D TIs, Bi_2Se_3 and Bi, were found by Bob Cava's group and the topological properties were investigated in collaboration with the Brookhaven National Laboratory and us [12]. Spin- and angle-resolved photoemission studies of a topological insulator $\text{Bi}_4\text{Se}_{2.6}\text{S}_{0.4}$ one member of the infinitely

adaptive series between elemental Bi and Bi_2Se_3 are presented in the paper. The compound, based on Bi_4Se_3 , is a 1:1 natural superlattice of alternating Bi_2 layers and Bi_2Se_3 layers; the inclusion of Se allows the growth of large crystals. The crystals cleave along the interfaces between the Bi_2 and Bi_2Se_3 layers, with the surfaces obtained having alternating Bi or Se termination. The resulting terraces, observed by photoemission electron microscopy, create avenues suitable for the study of one-dimensional topological physics. The electronic structure, determined by spin- and angle-resolved photoemission spectroscopy, shows the existence of a surface state that forms a large, hexagonally shaped Fermi surface around the Γ point of the surface Brillouin zone, with the spin structure indicating that this material is a topological insulator.

TIs are often excellent thermoelectric materials because similar features in the band structures are favorable for both properties [13]. Although the understanding of the direct theory behind this relationship is incomplete, the correlation between TIs and thermoelectric materials has guided the discovery of new TIs. However, excellent thermoelectric materials can be also topologically trivial (a compound is called topologically trivial if there is an even number of BI and thus no special surface state).

In reference [13] we propose new topological insulators in cerium-filled skutterudite (FS) compounds based on ab initio calculations. Most of them have been known as good thermoelectric materials and are under investigation in Yuri Grin's group together with Frank Steglich's team. The compounds have the chemical formula RT_4X_{12} (R = rare earth; T = Fe, Ru, or Os; and X = P, As, or Sb), in which heavy elements are expected to induce strong SOC. Similar to the half-Heusler compounds and Bi_2Se_3 , they are also known for excellent thermoelectric properties. We find that two compounds, $\text{CeOs}_4\text{As}_{12}$ and $\text{CeOs}_4\text{Sb}_{12}$, are zero gap materials with band inversions between Os-d and Ce-f orbitals, similar to HgTe. Both compounds are predicted to become topological Kondo insulators at low temperatures, which are Kondo insulators in the bulk but with robust Dirac surface states on the boundary. Furthermore, this family of topological insulators has more unique features. Due to similar lattice parameters there will be a good proximity effect with other superconducting FS compounds, which may realize Majorana fermions.

Additionally, the experimentally observed antiferromagnetic phase of $\text{CeOs}_4\text{Sb}_{12}$ at very low temperature provides a way to realize the massive Dirac fermion with topological magnetoelectric effects.

References

- [1] X.-L. Qi, S.-C. Zhang, *Physics Today* **63** (2010) 33.
- [2] L. Müchler, Haijun Zhang, Stanislav Chadov, B. Yan, F. Casper, J. Kübler, Shou-C. Zhang, C. Felser, *Angewandte Chemie* **51** (2012) 7221.
- [3] S. Chadov, X.-L. Qi, Jürgen Kübler, G. H. Fecher, C. Felser, and S.-C. Zhang, *Nature Mat.* **9** (2010) 541.
- [4] B. A. Bernevig, T. L. Hughes, and S.-C. Zhang, *Science* **314** (2006) 1757.
- [5] T. Graf, C. Felser, S. S. P. Parkin, *Prog. Solid State Chem.* **39** (2011) 1.
- [6] M. König, S. Wiedmann, C. Brüne, A. Roth, H. Buhmann, L. W. Molenkamp, X.-L. Qi and S.-C. Zhang, *Science*. **318** (2007) 766.
- [7] S. Ouardi, G. H. Fecher, C. Felser, J. Hamrle, K. Postava, and J. Pistora, *Appl. Phys. Lett.* **99** (2011) 211904.
- [8] H.-J. Zhang, S. Chadov, L. Müchler, B. Yan, X.-L. Qi, J. Kübler, S.-C. Zhang, and C. Felser, *Phys. Rev. Lett.* **106** (2011) 156402.
- [9] B. Yan, L. Müchler, C. Felser, *Phys. Rev. Lett.* 2012, in print.
- [10] X. Zhang, H. Zhang, C. Felser and S.-C. Zhang, *Science* **335** (2012) 1464.
- [11] Y. Xia, D. Qian, D. Hsieh, L. Wray, A. Pal, H. Lin, A. Bansil, D. Grauer, Y. S. Hor, R. J. Cava, and M. Z. Hasan, *Nature Phys.* **5** (2009) 398.
- [12] T. Valla, unpublished, arXiv:1208.2741
- [13] B. Yan, L. Müchler, X.-L. Qi, S.-C. Zhang, C. Felser, *Phys. Rev. B* **85** (2012) 165125.

¹ Johannes Gutenberg – Universität, Mainz, Germany.

² Department of Physics, Stanford University, Stanford CA, USA

³ Institut für Festkörperphysik, Technische Universität, Darmstadt, Germany.

Electronic Structure of Heusler Compounds with $C1_b$ Structure and “Zero Band Gap”

Siham Ouardi, Chandra Shekhar, Carlos E. Viol Barbosa, Shan Rong¹, Stuart S. P. Parkin¹, Gerhard H. Fecher, and Claudia Felser

Besides of the well-known wide range of properties of Heusler compounds [1], we have recently shown that many of the “heavy” Heusler semiconductors with 1:1:1 composition and $C1_b$ structure exhibit a zero band-gap behavior and are topological insulators induced by their inverted band structure [2]. In the present study, the electronic structure of the Heusler compounds PtYSb, PtLaBi, and PdLuBi was investigated by truly bulk sensitive, hard X-ray photoelectron spectroscopy (HAXPES). The measurements were performed for bulk samples as well as for thin films. The measured valence band spectra are clearly resolved and in well agreement to the first-principles calculations of the electronic structure of the compounds. The experimental results give clear evidence for the “zero band gap” state.

To identify the existence of the zero band gap behavior and topological states in Heusler compounds, a convenient experiment has to be carried out. HAXPES has emerged as a powerful tool to investigate the bulk electronic structure of materials in a variety of applied fields such as chemistry, physics, materials science and industrial applications [3]. The use of high-brilliance high-flux X-rays from the third-generation synchrotron radiation sources results in the emission of electrons having high kinetic energies, in turn leading to a high probing depth because of the increased electron mean free path [4]. Recently, several studies using high-resolution HAXPES have been realized. The electronic structure of solids like valence transitions in bulk systems as well as multilayer systems and the valence band of buried thin films have been investigated [5,6].

Polycrystalline samples of PtYSb and PtLaBi were synthesized by arc melting. The resulting ingots were post annealed in evacuated quartz tubes at 1073 K for two weeks. The composition and structure were checked by energy dispersive X-ray analysis and X-ray diffraction. Powder XRD revealed single phases with $C1_b$ structure for both compounds. The lattice parameters were determined to be 6.5256 Å and 6.8298 Å for PtYSb and

PtLaBi, respectively. The ingots were cut to sticks with a size of $(2 \times 2 \times 10)$ mm³ for further investigations of the thermoelectric properties and electronic structure. For the investigation by HAXPES, the sample sticks were fractured in-situ in a ultra-high vacuum chamber before each measurement to avoid contaminated surfaces that may appear during exposure to air.

For PdLuBi, thin film samples with the structure MgO(100) / Mo (2 nm) / Ta (20 nm) / Mo (1 nm) / PdLuBi (40 nm) / MgO (17 nm) were prepared by DC magnetron co-sputtering under Ar atmosphere. The composition of the PdLuBi thin films was analyzed by Rutherford backscattering spectrometry and particle-induced X-ray emission. The crystalline structure was examined by XRD. The surface morphology of the films was analyzed in-situ by reflection high energy electron diffraction. Ex-situ surface analysis was carried out by atomic force microscopy.

The HAXPES experiments were performed at the undulator beamlines BL15XU and BL47XU of SPring-8. At BL15XU, the photon energy was fixed at 5.9533 keV using a Si(111) double crystal monochromator (DCM) and the 333 reflection of a Si channel-cut post monochromator. At BL-47XU, the photon energy was fixed at 7.9392 keV using a Si(111) DCM and the 444 reflection of the post monochromator. The photoemitted electrons were analyzed for their kinetic energy and detected by means of a hemispherical analyzer (Scienta R4000–12 kV). The valence band spectra were taken with a total energy resolution of 140 meV or 240 meV as verified by spectra of the Gold Fermi energy. The sample temperature was set to 20 K in all measurements. For further details of the HAXPES experiment see References [7-10].

The electronic structures of PtYSb, PtLaBi, and PdLuBi have been calculated using the full potential all electron code Wien2k. Details of the calculations are described in References [11,12]. Spin orbit interaction was included for all atoms and LDA+*U* with the self-interaction correction double counting scheme for Lu. An effective Coulomb

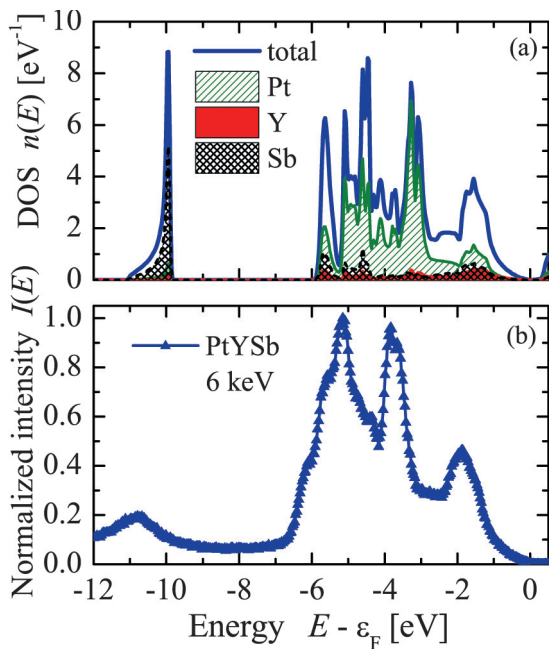


Fig. 1: Total and partial density of state (a) and valence band spectra (b) of PtYSb.

energy of $U_{\text{eff}} = U - J = 0.5$ Ry was used to reproduce the measured energy of the Lu 4f doublet. Relaxed lattice parameters were used in all calculations.

Figure 1 compares the calculated electronic structure of PtYSb to the measured valence band spectra. The structures in the valence band are clearly resolved and in good agreement to the calculated DOS. The low lying maximum at -11 eV arises from the s states localized at the main group element Sb. These states as well as the characteristic Heusler sp hybridization gap - separating s from p states localized at the main group element - are clearly resolved. The higher lying valence band (above -7 eV) of the compound shows clearly a structure with three major maxima. The first maximum at about -1.5 eV below ε_F emerges from d -states distributed at Pt as well as Y whereas the second, sharp maximum at about -3.5 eV arises from d states that are strongly localized at the Pt atoms only. The part of the valence band spectra below -4 eV appears smeared out. This energy region contains a mixture of s , p , and d states that contribute with different cross sections and therefore can not be easily related to the DOS. It is also stronger effected by life time broadening compared to energies close to ε_F . The effect of the photohole — electron correlation leads also to a shift of the observed

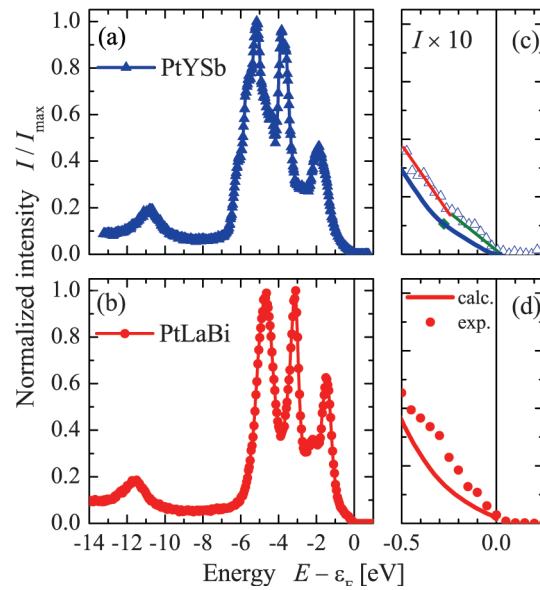


Fig. 2: Valence band spectra of PtYSb and PtLaBi. Panels (c) and (d) show the region close to the Fermi energy on an enlarged scale. The lines correspond to the DOS normalized to the maximum.

intensity maxima to lower energies compared to the corresponding maxima of the DOS. This shift is in average 0.3 eV at the first and 0.5 eV at the second maximum. These kinds of shifts were also found in narrow bandwidth valence band spectra of various other materials [13].

Figure 2 compares the measured valence band spectra of PtYSb (a) and PtLaBi (b). The spectra were taken with an excitation energy of about 5.9 keV. The maximum of the s states is shifted from about -10.7 eV to -11.6 eV when comparing the Y and the La containing compounds. The observed shift to lower energies when changing the composition is in good agreement to the calculations of the density of states. The width of the valence band exhibits the changes as expected from the calculated DOS. It is most narrow in PtLaBi and about 1 eV wider in PtYSb. Most interesting is the behavior of the spectra close to ε_F as shown in Figure 2(c and d). The intensities of PtYSb (2(c)) and PtLaBi (2(d)) exhibit a course as expected for a zero band gap insulator. Both, PtYSb and PtLaBi, exhibit a nearly linear behavior of the spectra and calculated DOS, as is expected for a cone type density appearing for linear dispersing bands. A bend of the DOS appears at the onset of the next lower valence bands at about -0.2 eV.

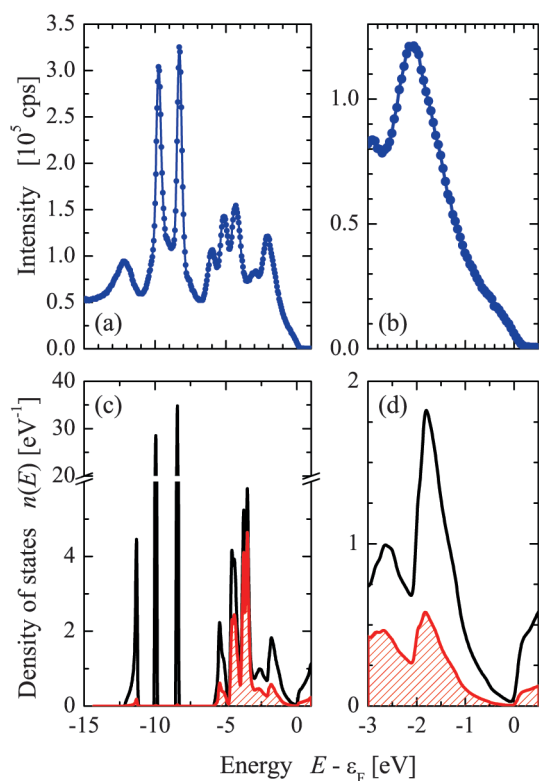


Fig. 3. Valence band of PdLuBi. (a)-(b) show the valence band spectra taken with a photon energy of about 8 keV. (c)-(d) show the density of states, the density localized at the Pd atoms is marked by the shaded area. (b) and (d) show the valence band close to the Fermi energy on an enlarged scale.

Valence band spectra of PdLuBi are presented in Figure 3 and compared to the calculated density of states. Figure 3(a) shows the valence band spectra excited by photons of about 8 keV energy. The high intensity with maximum between -13.5 eV and -11 eV corresponds to excitation of the low lying Bi s states as is seen by comparison to the density of states. The Lu $4f_{5/2}$ – $4f_{7/2}$ spin orbit doublet is found at energies of $E_{5/2} = -9.76$ eV and $E_{7/2} = -8.31$ eV. The spin orbit split Lu 4f states reside on top of states from the MgO protective overlayer that usually appear at about -9 eV. Such MgO states were previously also observed in the spectra from MgO covered Co_2MnSi [14]. The upper part of the valence band spectra above -6.5 eV exhibits the typical structure of the PdLuBi valence bands with four major maxima (-6 , -5.16 , -4.31 , -2.1 eV) and a smaller one at -2.9 eV. The splitting of the states at about -4 eV is not resolved in the spectrum. Slight energy differences between the maxima in the density of states and maxima of the spec-

trum are observed. These energy shifts are larger for states farer away from the Fermi energy (for example 0.3 eV at the -2.1 eV maximum and 0.6 eV at the -5.16 eV maximum). This is a typical effect of the photoemission process and emerges from the complex self energy of the photoelectrons interacting with the remaining $N - 1$ electron system. The spectra exhibit no clear cut-off at the Fermi energy as is observed when a metallic-type density is terminated by the Fermi-Dirac distribution but a rather smooth, linearly decreasing intensity is observed. A similar behavior was found in bulk materials of the “zero band gap” Heusler compounds PtYSb (see above) and PtLuSb [15].

We thank Eiji Ikenaga, Shigenori Ueda, and all the SPring-8 staff for their help during beamtimes. This research is financially supported by Deutsche Forschungsgemeinschaft (DFG) (project no. TP 1.3-A of Research Unit FOR 1464 ASPIMATT) and DfG-JST (project no. FE633/6-1). The HAX-PES measurements were performed at BL47XU of SPring-8 (Hyogo, Japan) with the approval of the Japan Synchrotron Radiation Research Institute (JASRI) (2011B1566, 2012A0043 and long-term Proposal 2008B0017) and at BL15XU of SPring-8 with the approval of NIMS (Nanonet Support Proposals 2010B4903).

References

- [1] T. Graf, C. Felser, S. S. P. Parkin, *Prog. Solid State Chem.* **39** (2011) 1.
- [2] S. Chadov, X. Qi, J. Kübler, G. H. Fecher, C. Felser, and S. Zhang, *Nature Mater* **9** (2010) 541.
- [3] K. Kobayashi, *Nucl. Instr. Meth. Phys. Res. A* **601** (2009) 32.
- [4] C. Dallera, L. Duo, L. Braicovich, G. Panaccione, G. Paolicelli, B. Cowie, and J. Zegenhagen, *Appl. Phys. Lett.* **85** (2004) 4532.
- [5] G. H. Fecher, B. Balke, A. Gloskowskii, S. Ouardi, C. Felser, T. Ishikawa, M. Yamamoto, Y. Yamashita, H. Yoshikawa, S. Ueda, and K. Kobayashi, *Appl. Phys. Lett.* **92** (2008) 193513.
- [6] S. Ouardi, G. H. Fecher, B. Balke, A. Beleanu, X. Kozina, G. Stryganyuk, C. Felser, W. Klöß, H. Schrader, F. Bernardi, J. Morais, and E. Ikenaga, *Phys. Rev B* **84** (2011) 155122.
- [7] S. Ouardi, C. Shekhar, G. H. Fecher, X. Kozina, G. Stryganyuk, C. Felser, S. Ueda, and K. Kobayashi, *Appl. Phys. Lett.* **98** (2011) 211901.
- [8] C. Shekhar, S. Ouardi, G. H. Fecher, A. K. Nayak, C. Felser, and E. Ikenaga, *Appl. Phys. Lett.* **100** (2012), 252109.

- [9] *S. Ouardi, G. H. Fecher, X. Kozina, G. Stryganyuk, B. Balke, C. Felser, E. Ikenaga, T. Sugiyama, N. Kawamura, M. Suzuki, and K. Kobayashi*, Phys. Rev. Lett. **107** (2011) 036402.
- [10] *X. Kozina, G. H. Fecher, G. Stryganyuk, S. Ouardi, B. Balke, C. Felser, G. Schönhense, E. Ikenaga, T. Sugiyama, N. Kawamura, M. Suzuki, T. Taira, T. Uemura, M. Yamamoto, H. Sukegawa, W. Wang, K. Inomata, and K. Kobayashi*, Phys. Rev. B **84** (2011) 054449.
- [11] *H. C. Kandpal, G. H. Fecher, and C. Felser*, J. Phys. D **40** (2007) 1507.
- [12] *S. Ouardi, G. H. Fecher, B. Balke, X. Kozina, G. Stryganyuk, C. Felser, S. Lowitzer, D. Ködderitzsch, H. Ebert, and E. Ikenaga*, Phys. Rev. B **82** (2010) 085108.
- [13] *K. Kobayashi*, Nucl. Instrum. Methods Phys. Res. A **547** (2005) 98.
- [14] *G. H. Fecher, B. Balke, A. Gloskowskii, S. Ouardi, C. Felser, T. Ishikawa, M. Yamamoto, Y. Yamashita, H. Yoshikawa, S. Ueda, and K. Kobayashi*, Appl. Phys. Lett. **92** (2008) 193513.
- [15] *C. Shekhar, S. Ouardi, G. H. Fecher, A. K. Nayak, C. Felser, and E. Ikenaga*, Appl. Phys. Lett. **100** (2012), 252109.

¹ IBM Almaden Research Center San Jose, CA 95120, USA.

Alkali-Metal Sesquioxides A_4O_6 ($A = \text{Rb}, \text{Cs}$): Electronic and Lattice Degrees of Freedom in Strongly Correlated p -Electron Systems

P. Adler, S. Chadov, G. H. Fecher, J. Kübler¹, S. Medvediev, C. Mühle², S. Naghavi, A. Sans², W. Schnelle, M. Jansen² and C. Felser

Alkali-metal hyperoxides with anionic paramagnetic O_2^- molecular units in the crystal structure have recently attracted considerable interest as their electronic behavior is reminiscent of the much-studied 3d transition-metal oxides [1]. The electronic properties of the hyperoxides are determined by the partially filled doubly degenerate $(\pi^*)^3$ electron configuration of the O_2^- units where the antibonding π^* orbitals are formed from the atomic O 2p orbitals. The $(\pi^*)^3$ configuration may be compared with the Jahn-Teller active $(e_g)^1$ and $(e_g)^3$ electron configurations encountered in Mn^{3+} and Cu^{2+} ions. The analogy to 3d systems suggests that a close interplay between electronic correlation, spin-orbital degrees of freedom and lattice instabilities may lead to a comparable variety of physical properties like magnetic, orbital and charge-ordering phenomena, insulator-metal transitions and even superconductivity. In fact, molecular oxygen itself is a prototype material for such behavior revealing antiferromagnetic order at ambient pressure and low temperature as well as pressure-driven transitions to metallic and superconducting states [2-4].

The molecular units are retained as O_2^- anions in the ionic crystal structures of alkali-metal hyperoxides AO_2 and sesquioxides $A_4\text{O}_6$. At ambient pressure the intermolecular interactions between the units are small. In the framework of a Mott-Hubbard-type description of the electronic structure the electronic correlation energy U is larger than the bandwidth W arising from intermolecular orbital overlap. The resulting magnetic properties of such electronically localized systems can be described by well-known concepts as Heisenberg exchange and the Goodenough-Kanamori rules [5]. In addition the rotational degree of freedom of the O_2^- anions is of crucial importance as it determines the exchange interactions. Orbital ordering induced by the reorientation of the molecular O_2^- units is considered as the driving force for the formation of a one-dimensional magnetic state in CsO_2 [6] which is quite comparable to the magnetic state realized in the cooperative Jahn-Teller system KCuF_3 .

Our own work concentrates on the alkali-metal sesquioxides $A_4\text{O}_6$ ($A = \text{Rb}, \text{Cs}$), the crystal structure of which per formula unit contains two paramagnetic hyperoxide O_2^- and one diamagnetic O_2^{2-} unit with completely filled $(\pi^*)^4$ shell (see Fig. 1). Formally the $A_4\text{O}_6$ compounds can be considered as anionic mixed-valence systems where electron transfer from the O_2^{2-} into the O_2^- units may be possible. Localization of the charges leads to a charge-ordered (CO) state. If a localization-delocalization transition could be induced by temperature it would be analogous to the well-known Verwey transition in magnetite (Fe_3O_4). The importance of electron correlations for the properties of the sesquioxides has been established in previous work. While electronic structure calculations on LSDA level predicted Rb_4O_6 to be a half-metallic ferromagnet [7], later work has demonstrated that Rb_4O_6 as well as Cs_4O_6 actually are magnetically frustrated systems without long-range magnetic order [8,9]. Electronic struc-

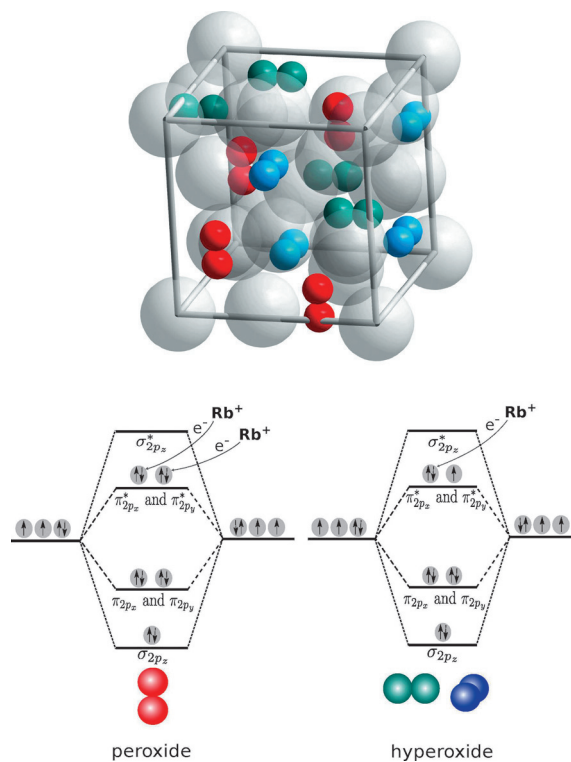


Fig. 1: Crystal structure and molecular orbital diagram for Rb_4O_6 (from Ref. [14])

ture calculations with proper incorporation of the electronic correlation effects lead to an insulating ground state where antiferromagnetic and ferromagnetic spin configurations have similar energies [10]. The magnetic properties of A_4O_6 differ from those of the pure hyperoxides which reveal antiferromagnetic order below 15 K and 10 K for RbO_2 and CsO_2 , respectively.

Our current work on A_4O_6 and related materials is integrated into the international research cluster LEMSUPER (Light Electron Molecular Superconductivity: An Interdisciplinary Approach) [11]. The cluster has been started in October 2011 and is funded by the EU Seventh Framework Programme (FP7) and the Japanese Science and Technology Agency. The present research has been initiated at the University of Mainz and is now continued at MPI-CPFS. Our research approach involves both, the synthesis of high-quality samples of A_4O_6 and related promising new materials and the characterization of their structural and physical properties at ambient and high pressure. Electronic structure calculations with appropriate incorporation of electronic correlations support the experimental work. Some recent results are presented in the following.

Magnetic Properties of Rb_4O_6 and Cs_4O_6

The magnetic properties of Rb_4O_6 and Cs_4O_6 have been established previously [8,9]. Considering more recent reports which suggest a close correlation between the orientational order of the dioxygen anions and the resulting magnetic states [6,12] we decided to reinvestigate the magnetic properties of A_4O_6 with special emphasis on the thermal protocol of the measurements. As an example we consider here data on Rb_4O_6 but similar results are obtained for Cs_4O_6 . In Fig. 2 (top) the temperature dependence of the molar magnetic susceptibility $\chi_m(T)$ is shown in an applied field of 7 T. As in previous work a divergence between $\chi_m(T)$ curves measured under zero-field cooled (ZFC) and field cooled (FC) conditions, suggests the absence of long-range magnetic order. The irreversibility sets in near 40 K. The shapes of the $\chi_m(T)$ curves are not typical for a spin-glass system, where the irreversibility between ZFC and FC curves occurs below a spin-freezing temperature. The latter is reflected in a cusp in the ZFC data. Below about 7 K there appears a ferromagnetic-like phase which is most prominently vis-

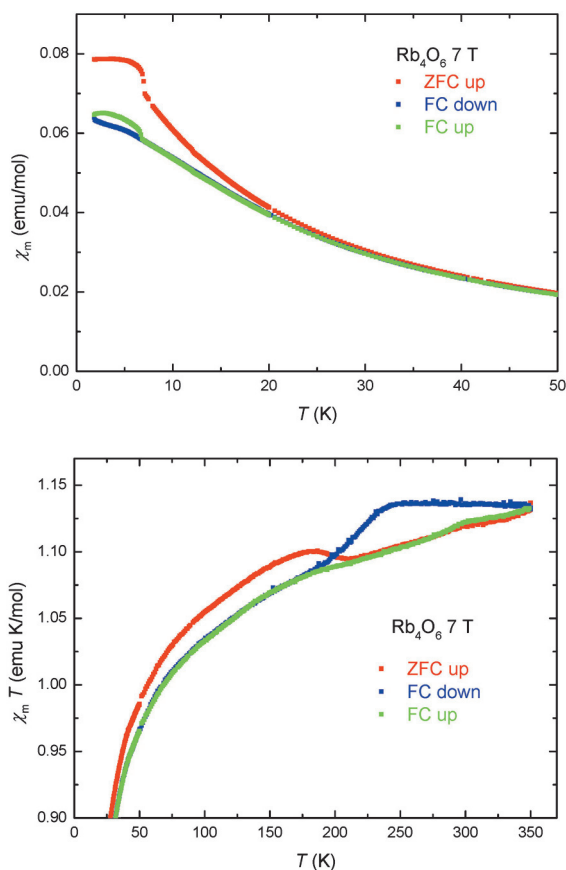


Fig. 2: Temperature dependence of the molar magnetic susceptibility χ_m (top) and the product $\chi_m T$ (bottom) for Rb_4O_6 .

ible in the ZFC curve measured after cooling down to 2 K. For fields > 1 T a saturated magnetization of $\sim 0.1 \mu_B$ /formula unit is observed. Curiously, the transition into this phase is almost invisible in the FC curve obtained during cooling in the applied field. However, due to a slow relaxation the magnetization is partially restored in the applied field. These effects are less visible in fields below ~ 1 T. The phase transition at ~ 7 K thus indicates the formation of ferromagnetic (or ferrimagnetic) domains with strong magneto-crystalline anisotropy. The domain formation, however, appears to be strongly dependent on the thermal history. This is in accord with recent observations on the phase $RbO_{1.72}$ where a cluster-glass state composed of ferromagnetic clusters in an antiferromagnetic (AF) matrix was postulated [12]. The cluster glass is formed only in rapid-cooling experiments, whereas it is absent if the sample is slowly cooled. The AF transition was deduced from a sharp maximum in the FC $\chi(T)$ curve. A comparable AF transition is not

seen in the Rb_4O_6 FC curve. Possibly the higher fraction of diamagnetic O_2^{2-} ions completely suppresses the AF order in Rb_4O_6 ($\text{RbO}_{1.5}$). For $\text{RbO}_{1.72}$ a structural transition near 230 K was observed which involves a reorientation of the O_2^{2-} anions [12]. The cooling rate through this transition was considered to determine the apparent magnetic behavior. A similar transition near 200 K may also occur for Rb_4O_6 and Cs_4O_6 . This is suggested by clear history-dependent anomalies in the magnetic susceptibility data in this temperature range, which for Rb_4O_6 are best seen in a representation of χT versus T (Fig. 2 bottom). Magnetic susceptibilities derived from EPR spectra of Cs_4O_6 show an anomaly near 200 K even more clearly [13].

Rb_4O_6 at High Pressure: A Theoretical Study

At ambient pressure the electronic system of Rb_4O_6 is essentially localized. Electronic structure calculations revealed, however, that the lowest energy excitation gap is not of the classical Mott-Hubbard-type with transitions from the lower into the upper Hubbard band, but rather of a charge-transfer type corresponding to excitations from the filled π^* orbitals of O_2^{2-} into partially filled orbitals of O_2^- [10]. Optical excitations of this type, which in the area of mixed-valence chemistry are known as intervalence bands, are possibly the origin for the black color of Rb_4O_6 . High pressure is a convenient way of tuning an electronic system from the strongly correlated ($U \gg W$) via a moderately correlated ($U \sim W$) to a non-correlated metallic ($U \ll W$) regime due to continuous shortening of the intermolecular distances. Much of the interesting physics in correlated materials just occurs in the $U \sim W$ regime where the transition from the insulating into a correlated metallic state is expected. The high-pressure behavior of Rb_4O_6 was studied by using the program CRYSTAL [14]. Electron correlation was taken into account by the hybrid correlation exchange functional B3YLP. In the low-pressure regime ($p < 75$ GPa) the system switches from an initial antiferromagnetic into a ferromagnetic insulating ground state. In this pressure range structural relaxation leads to symmetry lowering from cubic to tetragonal which corresponds to a CO state with discrete O_2^{2-} and O_2^- anions. Near 75 GPa the CO state is predicted to collapse and it is replaced by a half-metallic ferromagnetic state. The latter is

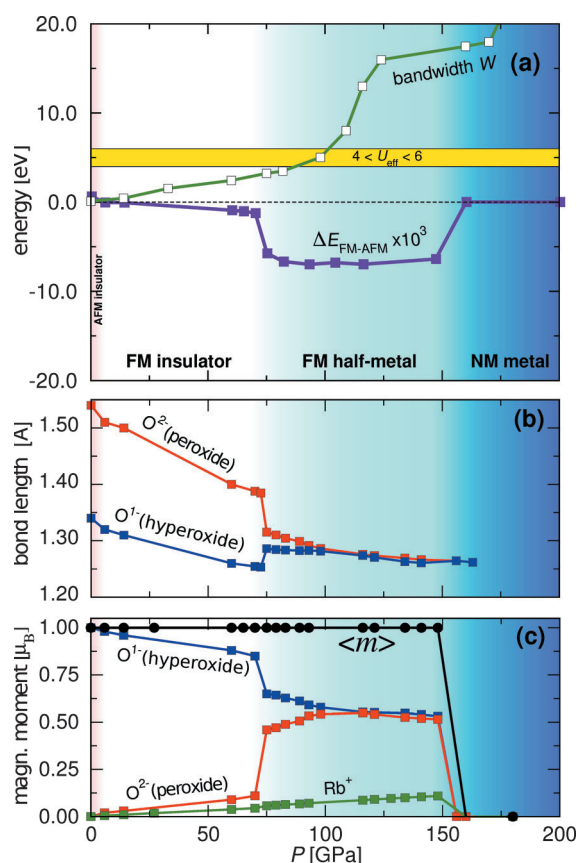


Fig. 3: Pressure evolution of electronic phases of Rb_4O_6 according to Ref. [14].

predicted to exist up to 150 GPa where the transition to a normal metallic non-magnetic state is expected. A summary of the relevant changes of properties under pressure as obtained from the calculations is depicted in Fig. 3. Note the equalization of the bond lengths and the concomitant averaging of the local magnetic moments near 75 GPa.

Rb_4O_6 and Cs_4O_6 at High Pressure: Experimental Results

The high-pressure behavior of Rb_4O_6 and Cs_4O_6 was studied by Raman spectroscopy at pressures up to 80 GPa (Fig. 4). Raman spectra at low pressures confirm the presence of peroxide and hyperoxide anions in Rb_4O_6 and Cs_4O_6 . For instance in Rb_4O_6 two peaks are found at Raman shifts of 795 and 1153 cm^{-1} . The former one corresponds to the stretching vibration of the peroxide anions and is in good agreement with the literature value of 782 cm^{-1} for Rb_2O_2 [15]. The high frequency peak

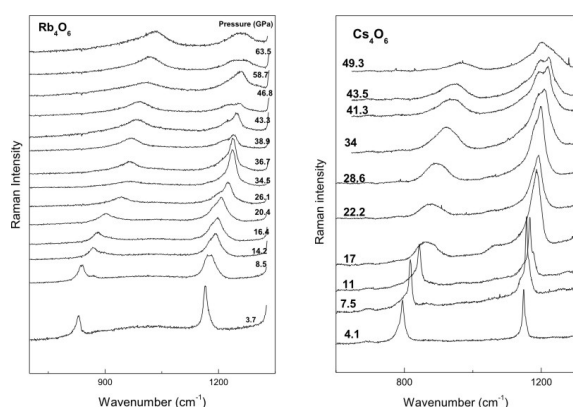


Fig. 4: Pressure evolution of Raman spectra of Rb_4O_6 (left panel) and Cs_4O_6 (right panel) at room temperature.

is assigned to the corresponding vibration of the hyperoxide anions and is comparable to the literature value of 1140 cm^{-1} for RbO_2 [16]. Both anions remain stable in both substances up to the highest pressures applied in this study. However, Raman spectra of Cs_4O_6 indicate a phase transition at pressures ~ 17 GPa. Strong broadening of the low-frequency Raman peak indicates that this transition is associated apparently with orientational disordering of peroxide anions. Similar broadening of the peroxide anion vibration peak in Rb_4O_6 is observable at pressures above 30 GPa. This phase transition unaccounted by previous theoretical studies may explain why no signs of metallization have been observed in our preliminary measurements of electrical resistivity of Cs_4O_6 up to 80 GPa and Rb_4O_6 up to 180 GPa. Combined structural, spectroscopic and electrical transport measurements in megabar pressure range are underway to clarify the pressure behavior of alkali sesquioxides.

Conclusions

The physical properties of the sesquioxides Rb_4O_6 and Cs_4O_6 are determined by strong electron correlations between the open shell 2p electrons and the orientational order of the O_2^{x-} units. At ambient pressure the electronic system is essentially localized and the magnetic state is determined by competing interactions. At high pressure crossover to more itinerant electron behavior is expected from our theoretical studies. However, preliminary high pressure studies indicate that pressure-induced orientational disorder of the O_2^{x-} anions may occur.

Future work will focus on chemical modifications, careful temperature dependent structural and further high pressure studies in order to explore the interplay between the electronic and lattice degrees of freedom in these correlated p-electron systems more deeply.

Acknowledgement

This work is financially supported by the international research program LEMSUPER [11].

References

- [1] A. K. Nandy, P. Mahadevan, P. Sen and D. D. Sarma, Phys. Rev. Lett. **105** (2010) 056403.
- [2] I. N. Goncharenko, O. L. Makarova and L. Ulivi, Phys. Rev. Lett. **93** (2004) 055502.
- [3] Y. Akahama, H. Kawamura, D. Häusermann, M. Hanfland and O. Shimamura, Phys. Rev. Lett. **74** (1995) 4690.
- [4] K. Shimizu, K. Suhara, M. Ikumo, M. I. Eremets and K. Amaya, Nature **393** (1998) 767.
- [5] K. Wohlfeld, M. Daghofer and A. M. Oles, Europhys. Lett. **96** (2011) 27001.
- [6] S. Riyadi, B. Zhang, R. A. de Groot, A. Caretta, P.H.M. van Loosdrecht, T. T. M. Palstra and G.R.Blake, Phys. Rev. Lett. **108**, (2012) 217206.
- [7] J. J. Attema, G. A. de Wijs, G. R. Blake and R. A. de Groot, J. Am. Chem. Soc. **127**(2005) 16325.
- [8] J. Winterlik, G. H. Fecher, C. Felser, C. Mühle and M. Jansen, J. Am. Chem. Soc. **129** (2007) 6990.
- [9] J. Winterlik, G. H. Fecher, C. A. Jenkins, S. Medvedev, C. Felser, J. Kübler, C. Mühle, K. Doll, M. Jansen, T. Palasyuk, I. Trojan, M. I. Eremets, and F. Emmerling, Phys. Rev. B **79** (2009) 214410.
- [10] J. Winterlik, G. H. Fecher, C. A. Jenkins, C. Felser, C. Mühle, K. Doll, M. Jansen, L. M. Sandratskii and J. Kübler, Phys. Rev. Lett. **102** (2009) 016401.
- [11] <http://www.lemsuper.eu>
- [12] S. Riyadi, S. Giryapura, R. A. de Groot, A. Caretta, P. H. M. van Loosdrecht, T. T. M. Palstra and G. R. Blake, Chem. Mater. **23** (2011) 1578.
- [13] K. Anderle and D. Arcon, unpublished results.
- [14] S. Naghavi, S. Chadov, C. Felser, G. H. Fecher, J. Kübler, K. Doll and M. Jansen, Phys. Rev. B **85** (2012) 205125.
- [15] H. H. Eysel and S. Thym, Z. Anorg. Allg. Chem. **411** (1975) 97.
- [16] J. B. Bates, M. H. Brooker, and G. E. Boyd, Chem. Phys. Lett. **16** (1972) 391.

¹ Institut für Festkörperphysik, Technische Universität Darmstadt, 64289 Darmstadt

² Max-Planck-Institut für Festkörperforschung, 70569 Stuttgart